Scilight

Environmental and Microbial Technology

https://www.sciltp.com/journals/emt

Review

Generation, Detection and Regulation Strategies of Reactive Species in Persulfate Activation Systems

Shizong Wang [1,2,*] and Jianlong Wang [1,2]

[1] Collaborative Innovation Center for Advanced Nuclear Energy Technology, INET, Tsinghua University, Beijing 100084, China
[2] Beijing Key Laboratory of Radioactive Wastes Treatment, Tsinghua University, Beijing 100084, China
* Correspondence: wsz2016@tsinghua.edu.cn

How To Cite: Wang, S.; Wang, J. Generation, Detection and Regulation Strategies of Reactive Species in Persulfate Activation Systems. *Environmental and Microbial Technology* **2026**, *1*(1), 8. https://doi.org/10.53941/emt.2026.100008

Received: 31 December 2025
Revised: 3 February 2026
Accepted: 5 February 2026
Published: 9 February 2026

Abstract: Persulfate-based advanced oxidation processes (AOPs) have emerged as highly promising technologies for degrading recalcitrant organic pollutants due to their flexible activation pathways and the diverse range of reactive species generated. This review establishes a comprehensive framework that encompasses mechanistic generation pathways, identification methods, and regulation strategies of both radical and non-radical species. Through this framework, the review reveals several fundamental challenges that hinder practical application, including uncertainties in identifying dominant reactive species in complex matrices, the intricate influence of coexisting ions and natural organic matter, catalyst deactivation under long-term operation, and the lack of sustainable and scalable synthesis routes for high-performance catalysts. In response to these issues, the review finally provides recommendations, such as integrating various characterization methods, developing predictive kinetic and computational models, engineering structurally robust and environmentally benign catalysts, and incorporating machine-learning tools to guide rational catalyst design and pathway prediction. These strategies outline clear future directions for advancing persulfate-based AOPs toward practical implementation. Overall, this work offers a systematic and insightful foundation that not only deepens mechanistic understanding but also bridges the gap between laboratory discoveries and real-world water treatment applications.

Keywords: persulfate activation; reactive species; identification; coordination structure; mechanism

1. Introduction

With the rapid development of industrialization and urbanization, the accumulation of trace organic pollutants in aquatic environments has become a global environmental issue, posing serious threats to ecosystems and human health [1,2].

Advanced oxidation processes (AOPs) have emerged as a promising strategy for the degradation of these persistent organics [3,4]. Among them, persulfate-based AOPs have garnered considerable attention. Compared to the conventional Fenton process, which is constrained by a narrow pH range and substantial iron sludge production [5,6], persulfate-based AOPs generates sulfate radicals ($SO_4^{\bullet-}$) with higher oxidation potentials (2.5–3.1 V), longer half-lives, and broader operational pH adaptability [7–9].

As depicted in Figure 1, research interest in persulfate-based AOPs, reflected by annual publication counts, has exhibited a continuous upward trend from 2015 through 2024, followed by a decline in 2025. This decline may be attributed to the persistent challenges that hinder their practical translation: (i) the frequent requirement of high catalyst dosages to achieve satisfactory degradation efficiency, raising economic and secondary pollution

concerns; (ii) the potential generation of acidic by-products, complicating post-treatment processes; and (iii) an incomplete mechanistic understanding, particularly regarding the role and regulation of diverse reactive species beyond $SO_4^{\bullet-}$ [10].

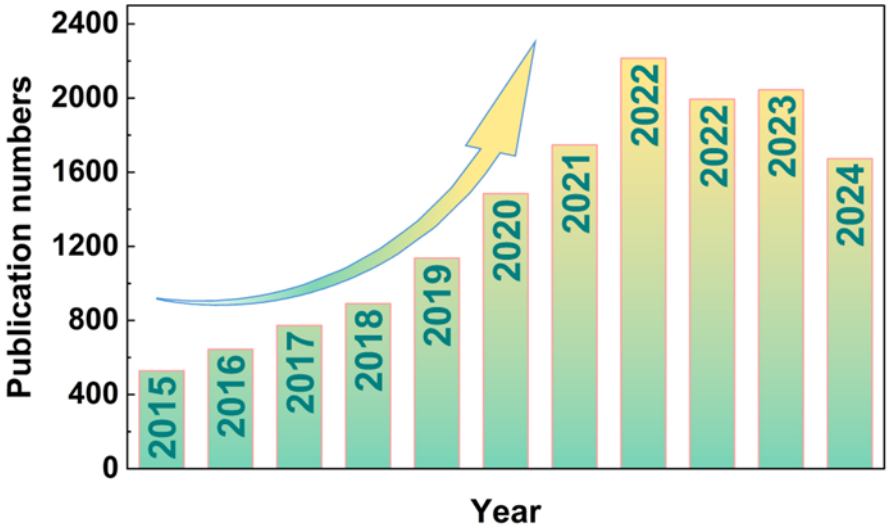

Figure 1. Publication numbers of persulfate activation with years.

As shown in Figure 2, the activation of persulfate (peroxymonosulfate, PMS, and peroxydisulfate, PDS) is now recognized to proceed through both radical and non-radical pathways. The latter encompasses singlet oxygen ($^1O_2$), surface-bound reactive complexes, high-valent metal-oxo species, and direct electron transfer processes [10–12]. For instance, nitrogen-doped carbons can activate PMS to form surface-confined reactive complexes [13], while tailored Co-N coordination structures can selectively generate $^1O_2$ [14]. These non-radical pathways often offer superior selectivity and better resistance to complex water matrices compared to radical-dominated reactions [15].

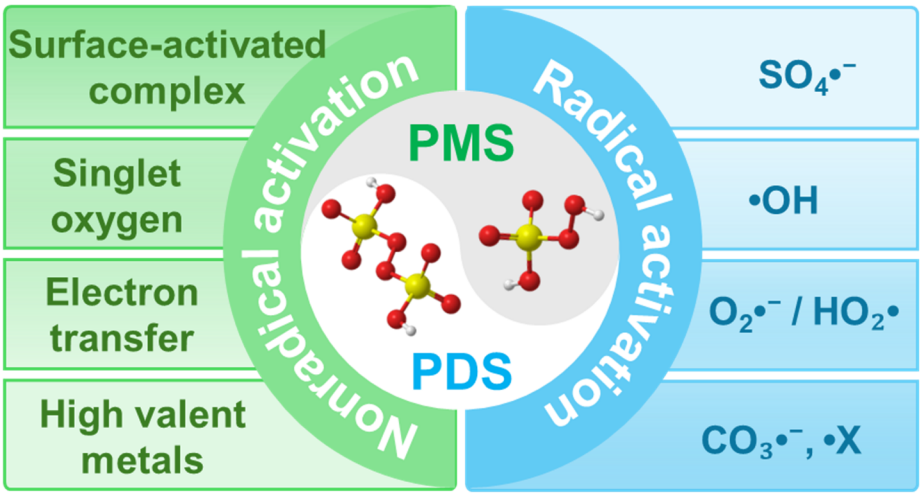

Figure 2. Reactive species generated by persulfate activation.

Despite extensive investigations, significant knowledge gaps and debates persist: (a) the coexistence and complex interplay (synergistic or competitive) of multiple radical and non-radical species under realistic conditions; (b) the lack of standardized and conclusive identification methodologies for differentiating these transient species; and (c) insufficient guidelines for the rational design of catalysts to steer the activation pathway toward a desired species for target pollutant removal. While previous reviews have catalogued catalysts for persulfate activation or summarized specific reaction types [16–19], a systematic review that critically links catalyst design to the precise generation and regulation of specific reactive species remains scarce.

This review aims to bridge this gap by providing a comprehensive and critical analysis of the generation mechanisms, identification techniques, and regulation strategies for reactive species in persulfate-based AOPs. Distinct from prior works, our specific objectives are: (1) to evaluate and compare advanced diagnostic tools (e.g.,

in-situ spectroscopy, chemical probing, computational studies) for unambiguous species identification; and (2) to propose design principles and modulation strategies (e.g., heteroatom doping, defect engineering, hybrid structure construction) to tailor reactive species generation for enhanced efficiency and selectivity.

By synthesizing the latest advances, this work offers new insights into the dynamic evolution and synergistic effects of reactive species in complex systems. It provides a forward-looking perspective on overcoming current identification ambiguities and presents a framework for the precise "customization" of catalytic sites to achieve predictable and controllable oxidation pathways. Ultimately, this review is intended to serve as a strategic guide for researchers to design next-generation, high-performance persulfate-based AOPs catalysts and to accelerate their application in practical water remediation.

2. Generation Mechanism of Reactive Species

Both PDS and PMS can be activated via either homogeneous or heterogeneous pathways. Homogeneous activation typically involves light irradiation, electrochemical methods, transition metal ions, plasma, and other energy inputs [20,21]. In contrast, heterogeneous activation primarily relies on catalysts such as transition metal oxides and single-atom catalysts [22,23]. The types of reactive species generated are closely related to the activation strategy. Due to the potential risk of secondary pollution associated with homogeneous activation, heterogeneous activation has emerged as the current research focus in the field of persulfate activation. In general, reactive species occurring in the process of persulfate activation are depicted in Figure 2.

2.1. Pathway of Radicals

(1) Sulfate radicals ($SO_4^{\bullet-}$)

The generation of $SO_4^{\bullet-}$ from PDS and PMS represents the primary activation step in persulfate-based advanced oxidation processes. Both oxidants contain relatively weak O-O bonds (bond dissociation energies of approximately 140 kJ·mol^{-1} for PDS and 140–210 kJ·mol^{-1} for PMS) that can be cleaved through thermal, photochemical, electrochemical, or catalytic activation. In PDS, the S-O-O-S linkage undergoes homolytic or single-electron cleavage to yield $SO_4^{\bullet-}$ as the dominant reactive species (Equations (1) and (2)), where the former produces two $SO_4^{\bullet-}$ radicals, and the latter generates one $SO_4^{\bullet-}$ together with SO_4^{2-} [24].

$$S_2O_8^{2-} \rightarrow 2SO_4^{\bullet-} \quad (1)$$

$$S_2O_8^{2-} + e^- \rightarrow SO_4^{\bullet-} + SO_4^{2-} \quad (2)$$

In PMS, the asymmetric S-O-O-H structure allows a more flexible activation process. Upon exposure to UV light, heat, transition metal ions (e.g., Fe^{2+}, Co^{2+}, Cu^{+}), or surface-active sites, PMS undergoes homolytic or single-electron cleavage to form $SO_4^{\bullet-}$ (Equation (3)), while heterolytic pathways can produce the transient $SO_5^{\bullet-}$ intermediate that further decomposes to $SO_4^{\bullet-}$ and •OH [25,26].

$$HSO_5^- + e^- \rightarrow SO_4^{\bullet-} + OH^- \quad (3)$$

(2) Hydroxyl radicals (HO•)

The generation of •OH from PDS and PMS involves both direct and indirect pathways that are highly dependent on the activation conditions. In the case of PDS, the initial homolytic or single-electron cleavage of the O-O bond produces $SO_4^{\bullet-}$ as primary oxidizing species [27], which can subsequently react with water molecules or hydroxide ions to yield •OH (Equations (4) and (5)).

$$SO_4^{\bullet-} + H_2O \rightarrow {\bullet}OH + HSO_4^- \quad (4)$$

$$SO_4^{\bullet-} + OH^- \rightarrow SO_4^{2-} + {\bullet}OH \quad (5)$$

This secondary conversion is favored under alkaline conditions, where the nucleophilicity of hydroxide promotes the transformation of $SO_4^{\bullet-}$ into •OH, leading to less selective but more powerful oxidation pathways.

Similar to PDS, PMS can also be activated by the two conversion pathways [28]. The homolytic cleavage of PMS yields both $SO_4^{\bullet-}$ and •OH directly, while heterolytic cleavage under basic or catalytic conditions facilitates the deprotonation of HSO_5^- and formation of $SO_5^{\bullet-}$ intermediates that further decompose to •OH [29,30].

Considering that $SO_4^{\bullet-}$ can be converted to •OH via H_2O molecules or hydroxyl ions, the direct formation of •OH thus becomes increasingly dominant in alkaline systems. In summary, the relative abundance of •OH versus $SO_4^{\bullet-}$ depends strongly on pH, activation mode, and the presence of catalytic or surface-active sites, which modulate the electron density distribution and the O-O bond cleavage route in both persulfate species [31–34].

(3) Superoxide radical (O_2•$^-$)

The generation of O_2•$^-$ during persulfate activation occurs through several indirect pathways, where it often acts as a secondary or intermediate species rather than a primary product of direct persulfate cleavage. First, O_2•$^-$ can be formed via the one-electron reduction of dissolved oxygen or through the transformation of other reactive intermediates. For instance, in carbonaceous catalyst systems, PMS can be oxidized to form SO_5•$^-$, which subsequently disproportionates to yield O_2•$^-$ and $^1O_2$ [35]. In addition, under alkaline conditions, base-catalyzed hydrolysis of PDS can also lead to O_2•$^-$ formation as part of a complex radical chain process [36]. Once generated, O_2•$^-$ may act as a precursor to other reactive species, such as •OH, through further transformation in the presence of protons or metal catalysts [37]. However, due to its relatively low redox potential and reactivity toward many organic contaminants, O_2•$^-$ often plays a secondary or mediating role rather than directly contributing to contaminant degradation [38]. Its involvement is highly dependent on the activation environment, including pH, catalyst type, and the presence of electron donors or transition metals, which can modulate the equilibrium between O_2•$^-$ and other oxygen-containing species [22,39].

2.2. Pathway of Non-Radical

2.2.1. Singlet Oxygen ($^1O_2$)

In recent years, studies have highlighted the significant role of $^1O_2$ as a key non-radical oxidant in the activation process of PDS and PMS. Unlike traditional radical-based pathways, the generation of $^1O_2$ through persulfate activation can occur via multiple mechanisms, including self-decomposition, catalyst-mediated processes, and radical recombination reactions [40]. For instance, under alkaline conditions, PMS can undergo self-decomposition to yield $^1O_2$, although this process is relatively slow [41]. The presence of quinones as catalysts significantly accelerates $^1O_2$ production via a complex pathway involving nucleophilic addition, dioxirane intermediate formation, and subsequent reaction with ionized PMS to regenerate the quinone and release $^1O_2$ [42]. Additionally, $^1O_2$ can be formed through the recombination of O_2•$^-$, which are generated during the base-catalyzed hydrolysis of persulfate anions [43]. Carbon-based catalysts with heteroatom doping such as nitrogen, have also been shown to activate PDS and PMS via non-radical pathways, where ketonic carbonyl groups or electron-deficient carbon sites facilitate the production of $^1O_2$ [44,45]. For instance, nitrogen-doped graphene and carbon nanotubes promote $^1O_2$ generation through electron transfer or by enhancing PMS self-decomposition [46].

2.2.2. Surface-Bound Reactive Complex

Recent evidence underscores the critical underestimated role of surface-bound PDS or PMS (denoted as PDS* or PMS*), a metastable complex formed via the interaction between persulfate and metal active sites where persulfate molecules coordinate with surface metal sites via the peroxide bond [47–49], leading to electron redistribution and O-O bond elongation that enhances its oxidative capability beyond free persulfate or $^1O_2$. Unlike freely diffusing radicals, surface-bound complexes exhibit enhanced oxidation potential and longevity, enabling efficient degradation of refractory organic compounds through direct electron transfer or hydrogen abstraction pathways. For instance, nickel phosphide/biochar can first adsorb PDS and activate PDS to produce PDS*, which exhibited excellent removal for tetracycline [50]. In addition, the oxidation potential of the PMS* depends on the metal types. For example, the study has shown that the oxidation potential of PMS* follows the order of Co-PMS > Mn-PMS > Ni-PMS [51].

2.2.3. High-Valent Metal-Oxo

In addition to surface-bound reactive complex, the generation of high-valent metal-oxo has been increasingly recognized as a significant pathway in persulfate activation, particularly in systems involving transition metal oxides. High-valent metal-oxo intermediates exhibit strong oxidative capacities and high selectivity toward electron-rich organic pollutants, operating primarily through non-radical mechanisms such as oxygen atom transfer (OAT) [52]. These species are typically formed via the interaction between persulfate and reducible metal centers (e.g., Co, Mn, or Fe) on catalyst surfaces, where persulfate acts as both an oxidant and an oxygen atom donor [53]. For instance, in Co-based PMS activation systems, the formation of Co(IV)=O has been proposed as a key intermediate, which demonstrates a higher redox potential than its precursor and facilitates selective oxidation of contaminants without generating significant free radicals [47,54]. Similarly, in Mn oxide-PMS systems, reactive manganese species such as Mn(V) and Mn(IV) contribute substantially to pollutant degradation, especially under acidic or neutral conditions where these intermediates remain stable and reactive [55]. Compared to conventional radical-based pathways, high-valent metal-oxo species offer advantages including reduced scavenging by

background water constituents, higher selectivity, and lower sensitivity to pH variations [52,56]. However, their formation and stability are highly dependent on the catalyst's structure, surface properties, and coordination environment [57].

2.2.4. Electron Transfer Process

In recent years, the electron-transfer process (ETP) has emerged as a dominant non-radical pathway in persulfate-AOPs, offering a unique mechanism for the selective degradation of organic contaminants [58]. Unlike conventional radical-based oxidation, ETP involves the direct transfer of electrons from organic pollutants to persulfate molecules adsorbed on the catalyst surface [59,60]. This process typically proceeds through the formation of surface-bound reactive complexes, which act as electron acceptors, while adsorbed organics serve as electron donors [61]. The oxidation efficiency in ETP systems is governed by the redox potential difference between the activated complexes and the target pollutants, enabling selective degradation of electron-rich compounds without significant interference from common water matrix components.

In metal-based systems, transition metal oxides such as CuO, Co_3O_4, and NiO have been widely reported to activate PDS via outer-sphere or inner-sphere interactions, leading to the formation of metastable surface complexes that mediate direct electron abstraction from co-adsorbed organics [62,63]. For instance, in CuO/PDS systems, ETP was identified as the primary pathway, where persulfate is reduced to SO_4^{2-} without cleavage of the O-O bond [64]. Similarly, in carbon-based systems, sp^2-hybridized carbon materials such as carbon nanotubes (CNTs) and nitrogen-doped carbons facilitate ETP by providing a conductive π-conjugated network that enhances electron shuttling from pollutants to persulfate [65]. The incorporation of nitrogen dopants, particularly graphitic N, further promotes persulfate adsorption and elevates the surface redox potential, thereby accelerating electron transfer [66,67].

A key advantage of ETP is its tunable oxidation capacity, which can be modulated by adjusting the catalyst's electronic structure, surface functionalization, or persulfate adsorption density [68]. Moreover, ETP exhibits high persulfate utilization efficiency and minimal susceptibility to scavenging by background anions or natural organic matter, making it particularly suitable for treating complex wastewater streams [69].

In addition, the ETP can also occur in the absence of catalysts. For example, PMS can degrade sulfonamides by ETP. The removal performance of sulfonamides by PMS is controlled by solution pH, PMS concentration and sulfonamides' concentration [69,70].

This electron-transfer-dominated oxidation pathway not only deepens the mechanistic understanding of persulfate chemistry but also provides a promising avenue for the development of selective and sustainable water treatment technologies.

3. Identification Methods of Reactive Species

The detection methods for reactive species are illustrated in Figure 3, and each of them is introduced in detail below.

3.1. Chemical Quenching and Probe Experiments

Chemical quenching and probe experiments have been widely employed as conventional methods for identifying reactive species in persulfate activation systems. In quenching tests, specific scavengers such as methanol, ethanol, tert-butyl alcohol, and furfuryl alcohol are introduced to selectively quench target species like $SO_4^{\bullet-}$, •OH, or $^1O_2$ [71,72]. However, the reliability of these scavengers is often compromised due to their lack of absolute specificity. For instance, tertiary butanol cannot only react with •OH, but also can inhibit the surface-reaction due to its high affinity on the surface of catalyst, which results in the misunderstanding of the role of •OH [73]. Similarly, sodium azide (NaN_3), a commonly used $^1O_2$ quencher, may also interact directly with persulfate, resulting in inaccurate conclusions [74]. Furfuryl alcohol, another commonly used $^1O_2$ quencher, cannot only react with $^1O_2$, but also with radicals [75], which would result in the overestimation of $^1O_2$. Methyl phenyl sulfoxide (PMSO), has been utilized to track high-valent metal-oxo species via its oxidation to methyl phenyl sulfone ($PMSO_2$) [76,77]. Nevertheless, this transformation can be induced by multiple oxidants, including Co(IV), Co(III)-PMS complexes, and even free radicals, limiting its diagnostic specificity. Similarly, traditional scavengers such as furfuryl alcohol and ethanol not only scavenge $^1O_2$ or $SO_4^{\bullet-}$ but also react readily with surface-bound reactive complexes, thereby obscuring the contribution of surface-bound reactive complexes [51,62].

To enhance the accuracy of reactive species identification, multi-probe and multi-quencher strategies have been proposed, where several probes or scavengers with complementary selectivity are applied simultaneously [78]. Furthermore, kinetic analysis of quenching and probe reactions, such as monitoring the time-dependent

formation of $PMSO_2$ or the decay of scavengers, provides deeper insights into the dynamic behavior and contributions of different reactive species [79,80]. Despite their practical convenience, chemical quenching and probe methods must be applied with caution and in conjunction with other in situ techniques (e.g., electron paramagnetic resonance spectrometer (EPR) to avoid misunderstanding and to construct a self-consistent mechanistic understanding of persulfate-based AOPs.

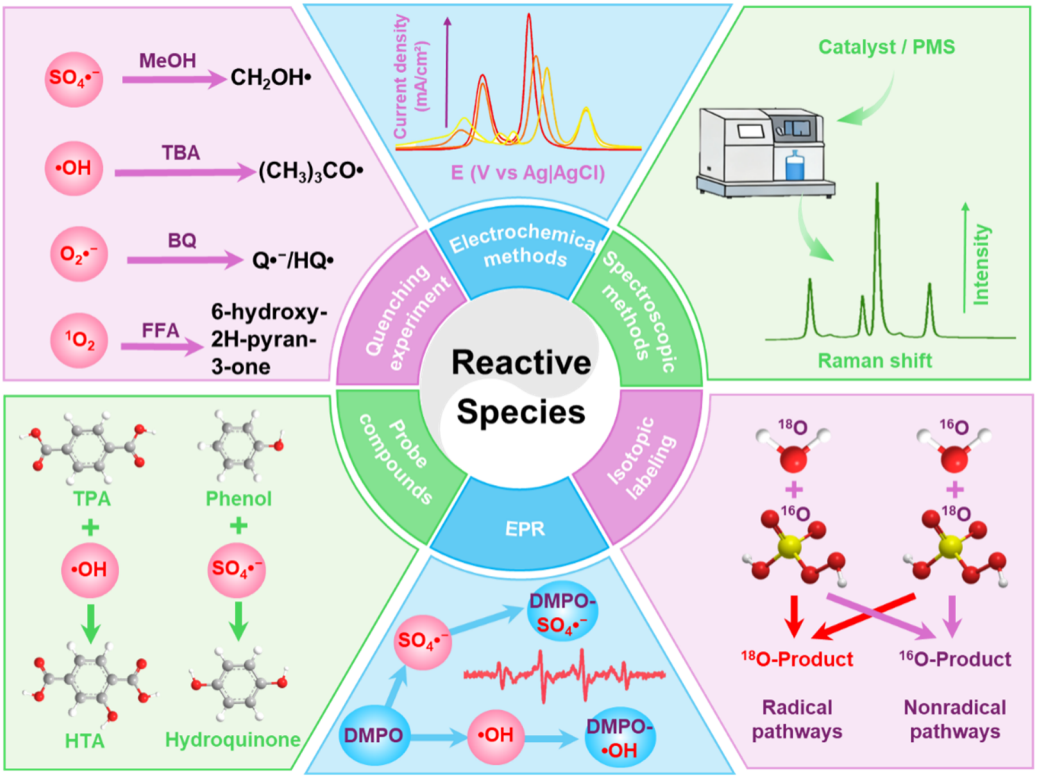

Figure 3. Identification methods of reactive species generated in AOPs.

3.2. EPR Technique

EPR spectroscopy is a powerful and widely applied technique for the detection, identification, and quantification of ROS and other radical intermediates in AOPs. Previous review has summarized the measurement conditions of EPR [81–83]. Commonly detected species include •OH, O_2•$^-$, SO_4•$^-$, and $^1O_2$. Figure 4 provided the spectra of the above reactive species. These short-lived radicals are typically stabilized and detected via spin trapping, wherein a transient radical reacts with a diamagnetic spin trap, commonly a nitrone or nitroso compound, to form a more persistent paramagnetic adduct measurable by EPR.

Among the most frequently used spin traps, 5,5-dimethyl-1-pyrroline N-oxide (DMPO) is widely employed to capture •OH, •SO_4^- and O_2•$^-$, forming DMPO-OH and DMPO-O_2^- adducts with characteristic EPR signatures. The $^1O_2$ is often detected using sterically hindered amine probes such as 2,2,6,6-tetramethylpiperidine (TEMP), 4-hydroxy-TEMP, or 4-oxo-TEMP, which yield stable nitroxide radicals (e.g., TEMPO, 4-OH-TEMPO) displaying distinctive triplet EPR signals. However, such nitroxide signals can also arise artifactually from oxidation by other reactive species (e.g., •OH or high-valent iron-oxo species), potentially leading to false-positive results [84]. Therefore, complementary techniques, such as near-infrared phosphorescence for $^1O_2$, solvent isotope substitution (e.g., D_2O), or chemical probes like 9,10-diphenylanthracene (DPA), are recommended to verify EPR findings and ensure accurate radical identification. For surface-bound reactive complexes, EPR measurements are typically performed with the catalyst retained in the solution, and the corresponding signal is recorded [12]. The same solution is then tested again after removing the catalyst; if no signal is detected in the second measurement, it indicates the presence of surface-bound reactive species that exist only when the catalyst is present. However, this approach cannot effectively distinguish between high-valent metal-oxo species and surface-bound complexes, leaving inherent limitations in mechanistic interpretation.

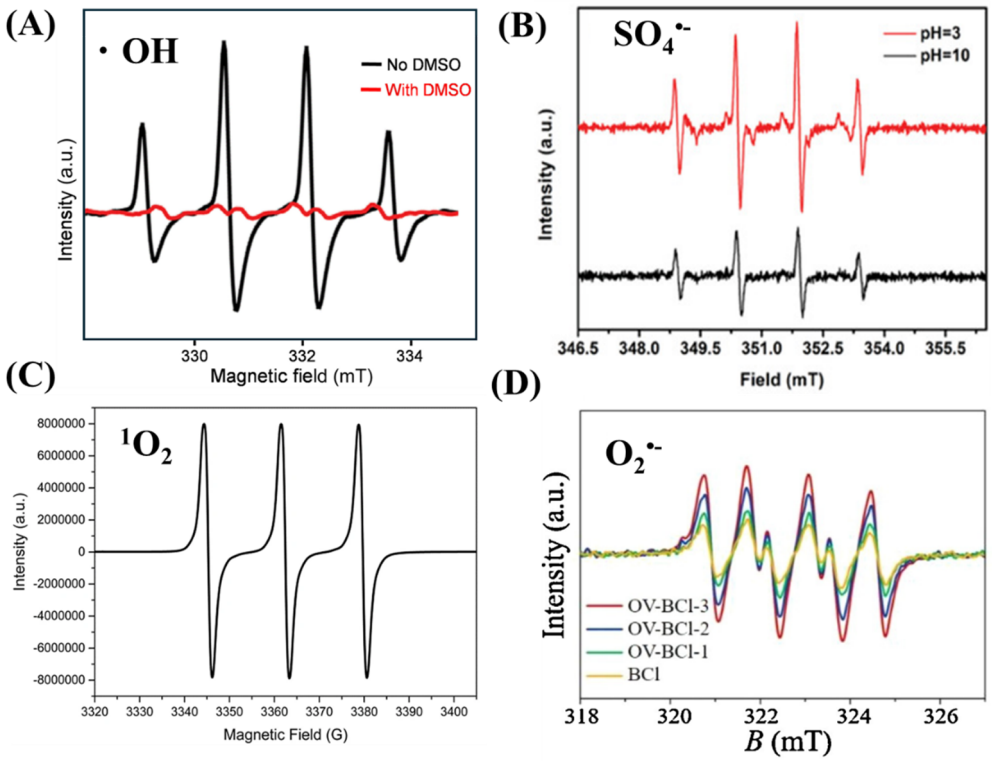

Figure 4. Spectra of common reactive species (**A**) HO• modified from [85]; (**B**) $SO_4^{\bullet-}$ modified from [86]; (**C**) $^1O_2$ modified from [87]; (**D**) $O_2^{\bullet-}$ modified from [88].

In addition to the above common ROS, some organic radicals can be also generated during the process of persulfate activation. EPR spin trapping can also characterize short-lived organic radicals such as carbon-centered (e.g., CH_3•) and phenoxyl radicals [83,89]. The DMPO-radical adducts typically yield six-line EPR spectra with hyperfine coupling constants of N ≈ 1.4–1.54 mT and H ≈ 2.0–2.28 mT, aiding radical identification. However, spectral overlap among different species, especially when using acyclic nitrones like polybutylene succinate, can complicate interpretation [90]. To enhance resolution, advanced spin traps such as fluorinated or phosphorylated nitrones have been developed. These generate more complex 12-line spectra due to ^{19}F or ^{31}P hyperfine splitting, improving radical discrimination [91]. For phenoxyl radicals, where overlapping spectra often obscure direct identification, complementary methods such as ^{31}P NMR or LC-MS analysis of TEMPO-type adducts provide structural confirmation [91,92].

Despite potential challenges related to spin adduct stability, competitive reactions, and interference from coexisting radicals, EPR spectroscopy when applied with suitable spin traps and corroborated by complementary analytical methods remains one of the most definitive and insightful techniques for elucidating the nature, dynamics, and mechanistic roles of radical species in AOPs.

3.3. Spectroscopic and Electrochemical Methods

Chromatographic techniques such as ultra-high-performance liquid chromatography coupled with mass spectrometry (UPLC-MS) are used to identify specific oxidation products derived from radical reactions. For example, the reaction between $^1O_2$ and 9,10-diphenylanthracene (DPA) forms a characteristic endoperoxide ($DPAO_2$), which can be quantified by UPLC-MS to confirm $^1O_2$ generation [93]. Similarly, a variety of chemical probes can be used to confirm •OH generation through the formation of characteristic reaction products. For example, the reaction between •OH and terephthalic acid forms the fluorescent product 2-hydroxyterephthalic acid [94], which can be quantified by fluorescence spectroscopy or UPLC-MS. Additionally, •OH reacts with p-hydroxybenzoic acid to produce specific dihydroxybenzoic acids such as 2,5- dihydroxybenzoic acids and 3,4-dihydroxybenzoic acids [95], while its reaction with salicylic acid yields 2,3- and 2,5-dihydroxybenzoic acids [96]; both sets of products can be detected by HPLC or UPLC-MS. Benzoic acid can also serve as a probe, forming o-, m-, and p-hydroxybenzoic acids upon •OH attack [97]. Fluorescent probes such as dihydrofluorescein and dihydrorhodamine 123 are oxidized by •OH to produce dichlorofluorescein and rhodamine 123, respectively, which can be quantified by fluorescence spectroscopy [98].

For $SO_4^{\bullet-}$, the probe compounds used for •OH such as methanol, ethanol and benzoic acid can be also used to generate formaldehyde, acetaldehyde, hydroxybenzoic acids or methoxyphenols [99,100], respectively, which can be quantified by HPLC or GC-MS. However, when •OH and $SO_4^{\bullet-}$ coexisted in the system, their unambiguous identification requires additional support from EPR measurements, kinetic analysis, or the use of multiple complementary probe compounds.

Several selective probes are widely used to verify the generation of $O_2^{\bullet-}$ by monitoring their specific reduction or oxidation products. Nitro blue tetrazolium is one of the most common probes, as $O_2^{\bullet-}$ readily reduces nitro blue tetrazolium to form the intensely colored formazan, which can be quantified by UV-Vis spectroscopy [101]. Similarly, the reaction between $O_2^{\bullet-}$ and cytochrome c produces its reduced form, ferrocytochrome c, which can be detected spectrophotometrically [102]. Hydroethidine is another well-known probe, undergoing $O_2^{\bullet-}$ specific oxidation to form 2-hydroxyethidium, a fluorescent product detectable by LC-MS or fluorescence spectroscopy [103]. Additionally, luminol chemiluminescence offers a highly sensitive route, as its reaction with $O_2^{\bullet-}$ produces characteristic luminescence that can be monitored to confirm radical generation [104].

As described in Section 2.2.4, ETP involves direct electron transfer from pollutants to surface-adsorbed persulfate. Electrochemical methods offer direct and in-situ means to characterize this pathway. Electrochemistry method is usually used to characterize the presence of surface-bound complex and the electron transfer mechanism. By monitoring the positive shift in the open-circuit potential of the catalyst before and after the addition of persulfate, it can provide key evidence for confirming the formation of surface-bound complexes. The fundamental principle is that when persulfate forms an activated surface complex via coordination or electron transfer on the catalyst surface, it alters the energy level at the electrode/solution interface, thereby enhancing its apparent oxidation potential, which macroscopically manifests as an increase in the open-circuit potential [105]. A significant advantage of this method is its ability to directly and in-situ reflect the generation of surface-active complexes and their relative oxidative strength, effectively avoiding the misinterpretations caused by side reactions between traditional scavengers and the target complexes. However, its main limitation is that it usually only provides semi-quantitative comparative results, making it difficult to precisely determine the absolute concentration of the surface complexes. Furthermore, the signal represents an integrated response from the entire surface, offering limited resolution of the specific atomic-scale structure and formation sites of the complexes.

The galvanic oxidation process (GOP) is a commonly employed device for evaluating direct electron transfer (DET) processes in heterogeneous oxidation systems (Figure 5). In a typical GOP configuration, two dissimilar conductive materials are electrically connected but immersed in the same electrolyte without external power input, thereby forming a spontaneous galvanic pair [106]. The potential difference between the two electrodes drives electron flow across the interface, allowing reactive species generated at the anode surface to be directly attributed to DET rather than to mediated oxidation pathways. By monitoring changes in electrode potential, current response, or the formation of characteristic oxidation products, the GOP enables quantitative assessment of electron-transfer efficiency and surface reactivity. The major advantage of this approach lies in its simplicity, intrinsic energy-free operation, and ability to isolate DET from radical-mediated processes. However, its performance may be affected by solution conductivity, electrode passivation, and competitive radical pathways, which can obscure the contribution of pure DET. In addition, the galvanic coupling is material-dependent, limiting its applicability across systems with complex redox equilibria.

3.4. Isotopic Labeling and In Situ Characterization Techniques

Isotope techniques, combined with advanced in situ spectroscopic methods, provide a powerful and non-invasive strategy for identifying active species and unraveling complex reaction mechanisms in catalytic water treatment and energy conversion systems [107]. The fundamental principle relies on the preferential cleavage of bonds containing light isotopes (e.g., ^{12}C or ^{1}H), which leads to the enrichment of heavy isotopes (e.g., ^{13}C or ^{2}H) in the residual substrate. The resulting enrichment factors (ε) and the correlation between carbon and hydrogen isotope fractionation ($\Lambda=\Delta\delta^{2}H/\Delta\delta^{13}C$) serve as a distinctive "molecular fingerprint" to discriminate between different reaction pathways and identify the dominant reactive species. For instance, in the degradation of diethyl phthalate by zero-valent iron-activated persulfate, a characteristic dual-isotope plot with a stable Λ value of ~11–13 across different pH conditions provided direct evidence for a mechanism involving •OH addition to the aromatic ring [108], corroborating findings from quenching experiments and EPR. This was further supported by apparent kinetic isotope effect (AKIE) values (^{13}C-AKIE ~1.01–1.02 and ^{2}H-AKIE~1.14–1.40), which confirmed C-H bond cleavage as the rate-limiting step, which is consistent with the formation of hydroxylated intermediates. A key advantage of this method is its ability to circumvent ambiguities associated with traditional scavenger tests, where quenchers can non-selectively react with multiple species like surface-bound complexes, $\bullet SO_4^-$, and •OH. By

providing direct evidence of the reaction site and bond cleavage, this method offers an unambiguous line of evidence to verify the dominant reactive species and delineate complex transformation pathways, thereby significantly advancing our mechanistic understanding of advanced oxidation processes and providing a critical foundation for assessing contaminant fate and remediation efficacy in real-world environments.

Using time-resolved in situ attenuated total reflectance infrared (ATR-IR) spectroscopy, key intermediates such as Co(IV)=O, O-Co(III)-O^{-}, and OOH were directly observed [109]. This combination of isotope labeling, in situ IR, and kinetic isotope effect analysis enables real-time tracking of interfacial states and transient intermediates, offering unprecedented insights into active site identity and reaction pathways in complex aqueous catalytic systems [110].

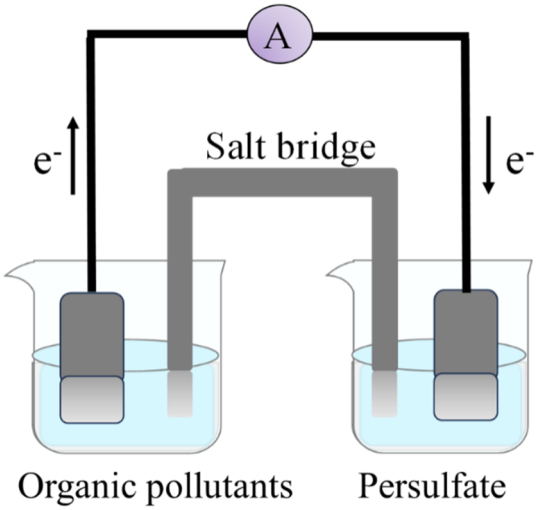

Figure 5. Diagram of GOP experimental device.

4. Regulation Strategies for Reactive Species Generation

This chapter examines key strategies for regulating reactive species generation in heterogeneous persulfate activation systems. While carbon-based materials are among the most widely studied and applied catalysts in this field [31,111,112], the principles discussed including catalyst structure design, functionalization, and reaction condition control are broadly applicable across various catalytic platforms. For clarity, Section 4.2 focuses specifically on the functionalization of carbon-based catalysts, whereas Sections 4.1 and 4.3 address general regulatory mechanisms illustrated with representative carbon and non-carbon examples. The reactive species generated during persulfate activation are influenced by multiple factors, as illustrated in Figure 6. The following sections provide a detailed discussion of each factor.

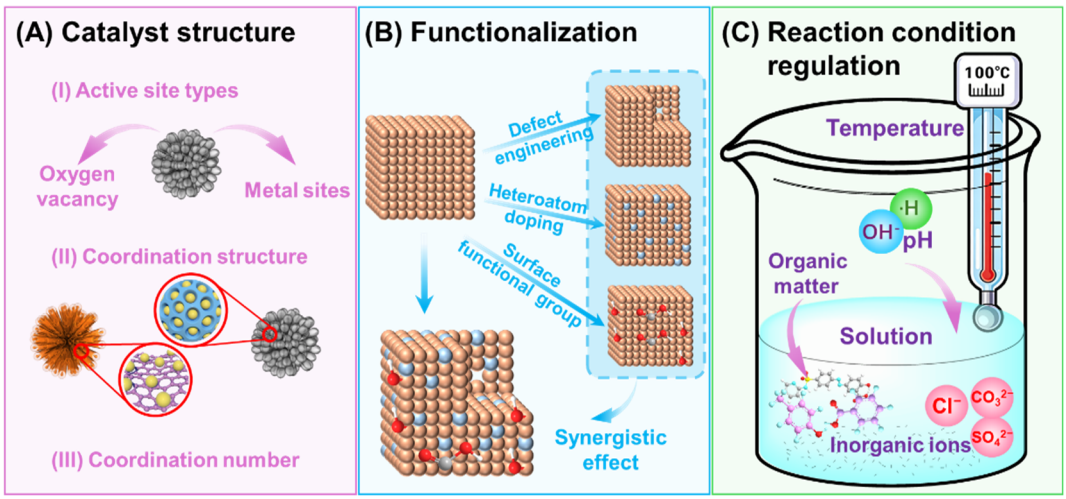

Figure 6. Regulation strategies for reactive species generation in the process of persulfate activation.

4.1. Catalyst Structure Regulation

The type of metal active site in catalysts such as carbon-based metal oxides or single-atom catalysts (SACs) plays a decisive role in modulating both the catalytic activity and reaction pathways in persulfate-based AOPs. Transition metals such as Fe, Co, Cu, and Mn, with their unique electronic configurations and partially filled d-orbitals, exhibit distinct behaviors in persulfate activation. For instance, Cu-based SACs with lower coordination numbers (e.g., Cu-N_2) demonstrate enhanced catalytic activity due to their unsaturated electronic state and higher charge density, which facilitate electron transfer and reduce the energy barrier for PDS dissociation into $SO_4^{\bullet-}$ [113]. In contrast, Fe and Co SACs often promote the formation of high-valent metal-oxo species (e.g., Fe(IV)=O or Co(IV)=O) through a non-radical pathway, especially when coordinated in symmetric M-N_4 configurations [114,115]. This regulation of the metal center's chemical environment can be precisely achieved by using modified supports. A prime example is the use of UiO-66-X MOFs as carriers for iron oxide nanoparticles (FeO_x@UiO-66-X). Introducing electron-donating groups (e.g., -NH_2, -OH) on the ligand increases the charge density around Fe, lengthens the Fe-O bond (from 2.06 Å to 2.12 Å), and favors a single-electron transfer pathway, leading to dominant •OH radical generation. Conversely, electron-withdrawing groups (e.g., -NO_2, -F) decrease the Fe charge density, shorten the Fe-O bond to 1.99 Å, and steer the reaction towards a two-electron transfer process, facilitating the formation of high-valent Fe(IV)=O [116]. Beyond carbon supports, alternative materials like silicon carbide (SiC) offer unique coordination environments. For example, a Co single-atom catalyst with a unique Co-Si_5 coordination structure was shown to preferentially activate PMS via a non-radical pathway. This Co-Si coordination enhances electron transfer and lowers the energy barrier, leading to the dominant formation of surface-bound reactive complexes and high-valent Co(IV)=O, which exhibit superior performance and resistance to inorganic anions in complex wastewater [117]. The spin state of the metal center, influenced by the coordination environment and ligand field, further fine-tunes the catalytic behavior: high-spin states favor radical generation, while low- or intermediate-spin states promote electron-transfer processes or high-valent species formation [118]. Furthermore, the coordination atoms can also alter the persulfate activation pathway resulting in the generation of different reactive species. For instance, CoN_2O_2 activated PMS to form surface-bound complexes [118], while CoB_1N_3 resulted in the generation of high-valent cobalt-oxo [119]. Similarly, the coordination number can also regulate the type of reactive species. Compared to CoN_2O_2, CoN_1O_2 induced the formation of high-valent cobalt-oxo instead of surface-bound complexes [120]. Furthermore, the size of active center has been demonstrated to modulate the type of reactive species. When the size of active center is nano level, PMS was activated to generate radicals, while PMS was activated to produce non-radicals when the size of active center was single atom [121]. Therefore, by rationally designing the metal coordination structure including the coordination number, the identity of coordinating atoms (e.g., N, O, Si), and the electronic properties of the support, the catalytic reaction pathway can be strategically controlled, enabling a switch between radical-dominated and high-valent metal-oxo-dominated mechanisms for efficient pollutant degradation across diverse water matrices.

Although this section includes examples from both carbon and non-carbon catalysts (e.g., SiC-supported Co SAC), the underlying principles such as coordination environment tuning, metal center selection, and spin state manipulation are universal design strategies for regulating persulfate activation pathways.

4.2. Functionalization of Carbon-Based Catalysts

In addition to modulation of catalyst structure, functionalization plays a crucial role in regulating the generation of reactive species. Carbon-based catalysts have been extensively investigated owing to their low cost, structural diversity, and highly tunable physicochemical properties, rendering functionalization a particularly effective strategy for performance optimization. Accordingly, given their extensive investigation and high tunability, this section focuses on the functionalization of carbon-based catalysts, which can be broadly classified into defect engineering, heteroatom doping, and surface functional group modification

(1) Defect engineering

In persulfate-based AOPs, defect engineering has been demonstrated as an effective strategy to significantly regulate the physicochemical properties of catalysts and enhance their activation performance [122,123]. The presence of defects such as vacancies or grain boundaries disrupts the periodic lattice structure of materials, leading to local charge redistribution, alterations in electronic structure, and the formation of unsaturated coordinated atoms [124]. These changes generate high-energy active sites on the catalyst surface. Such structural modifications not only strengthen the adsorption of persulfates but also promote electron transfer, modulate band structures, induce surface reconstruction, and even act as anchoring sites for constructing new active centers, such as single-atom sites.

Taking oxygen vacancies (OVs) as an example, OVs can be introduced into metal oxides through heat treatment, doping, or chemical etching. OVs effectively tune the electronic structure, enhance persulfate adsorption, facilitate O-O bond elongation, lower reaction energy barriers, and promote the generation of both radical and non-radical reactive species [125,126]. In addition to persulfate, OVs can serve as electron donors to promote O_2 adsorption and activation, induce the formation of $^1O_2$, and interact with dissolved oxygen to form surface-bound reactive complexes, further improving pollutant degradation efficiency [127]. In this case, its presence enhanced the generation of reactive species by both promoting persulfate activation and facilitating oxygen activation. Furthermore, the adequate oxygen and sulfur dual vacancies can further facilitate the PDS activation by regulating the electron delocalization and lowering the charge transfer energy [128].

Beyond OVs, other anionic vacancies such as nitrogen vacancies (NVs), sulfur vacancies (SVs), and selenium vacancies (SeVs), as well as cationic vacancies such as titanium vacancies (TiVs), have also been extensively investigated. For instance, introducing NVs into g-C_3N_4 creates electron-rich regions that enhance PMS adsorption and activation, thereby promoting the co-generation of •OH and $^1O_2$ [129]. In MoS_2, constructing SVs improves its electron transfer capability toward PMS, significantly enhancing the degradation performance toward tetracycline [130].

Structural defects or heteroatom doping in carbon materials likewise enhance their affinity for persulfates and facilitate electron-transfer reactions in non-radical pathways. For example, defect-rich carbon nanotubes (CNTs-VD) can transfer more electrons during PMS activation than pristine CNTs, resulting in more efficient degradation of organic contaminants [131].

Overall, the density, type, and spatial distribution of defects exert substantial influence on catalytic activity. An optimal defect concentration generally improves reaction kinetics, whereas excessive defects may compromise structural stability and suppress catalytic performance. Therefore, precise regulation of defect structures through control of heat-treatment temperature, dopant types, etching methods, and other parameters enables directional modulation of persulfate activation pathways and enhances the degradation efficiency and selectivity toward trace water contaminants [132]. A recent study reported an ionizing-radiation-regulated defect engineering method that can tune the defect degree by controlling the irradiation conditions [133]. Although this approach may offer a simple route for regulating catalyst defects, it is still in its infancy, and further studies are needed to clarify how to precisely control the defect type.

(2) Heteroatom doping

It should be noted that elemental doping may sometimes alter the coordination structure of the active sites, but it may also leave the coordination environment unchanged and instead modify the material's electronegativity. In the previous section on coordination structures (Section 4.1), we discussed how element regulation can influence the coordination environment. Here, however, the term "doping" mainly refers to its role in adjusting the surface charge properties of the catalyst. Incorporating heteroatoms such as N, S, B, and O into the carbon lattice effectively modulates its electronic structure and surface charge distribution [134].

Heteroatom doping can be categorized into metal-heteroatom doping and non-metal-heteroatom doping. Common non-metal heteroatom includes N, O, S, C, B and P. Among them, nitrogen doping has been widely investigated. Nitrogen doping introduces graphitic, pyridinic, or pyrrolic N species that enhance electrical conductivity and create positively charged sites favorable for persulfate adsorption and activation [135–137]. Graphitic N, in particular, promotes non-radical electron transfer mechanisms (see Section 2.2.4) by stabilizing surface complexes with persulfate species [138,139]. In a previous study, it was reported that N-doped graphene activated PMS to produce both •OH and SO_4•$^-$ as well as persistent free radicals as [140,141], while other studies showed that N-doped carbon materials tended to activate PMS to produce non-radicals such as $^1O_2$ and to induce the electron transfer between PMS and organic pollutants [105,142,143]. Co-doping often produces synergistic effects, optimizing the catalytic sites and enhancing pollutant degradation efficiency [144,145]. For instance, S and B doping altered the electron density of neighboring carbon atoms, improving redox activity and facilitating charge transfer [146,147].

It is noted that some studies showed that the content of non-metal heteroatoms determines the catalytic activity of catalysts [148,149], while other studies show that there is an optimal content for the non-metal heteroatoms [54,133]. In addition, the study has shown that the catalytic activity for PDS was determined to not only be related to the contents of heteroatom dopants (B and N), but also the positions of B and N in the co-doping configurations [150]. Collectively, these studies suggest that the catalytic performance toward persulfate activation is governed by both the content and the doping configuration of non-metal heteroatoms, with an optimal dopant level rather than a monotonically increasing effect.

Common metal heteroatoms include transient and precious metals. For instance, carbon nanotubes encapsulated with nickel nanoparticles significantly increased the adsorption and catalytic activity for PDS [151]. Ruthenium (Ru) doped carbon nitride resulted in the formation of Ru-N_2 that exhibited good catalytic activity and stability for PMS [152]. In general, metal doping can significantly enhance the catalytic activity of catalysts toward persulfate activation. However, after metal incorporation, the persulfate activation pathway is primarily governed by the coordination environment of the metal active sites, as discussed in Section 4.1.

Another common strategy is to further increase the density of metal active sites in existing carbon-supported metal composites by constructing dual-metal active sites. Typically, such dual-metal sites are formed in a single step during the calcination process. Recent studies have reported an alternative approach in which a second type of metal active site is generated in situ on the surface of SAC-Co through ionizing irradiation, thereby forming dual-metal active sites. The introduction of this secondary metal site not only enhances the catalytic activity but also alters the persulfate activation pathway [153]. The activation pathway evolved from Co(IV)=O to surface-confined reactive species.

(3) Surface functional groups

Oxygen-containing functional groups such as hydroxyl (-OH), carboxyl (-COOH), and carbonyl (C=O) play a vital role in persulfate activation [154,155]. Among them, C=O groups have been identified as key active sites that can generate $^1O_2$, leading to efficient non-radical oxidation pathways [156]. These functional groups also improve pollutant adsorption through hydrogen bonding and electrostatic interactions [157,158]. For instance, increasing the content of acidic oxygen functional groups improved the catalytic activity of granular activated carbon for persulfate [159]. However, excessive oxygen functionalities may increase surface negativity, hindering persulfate adsorption and electron transfer [158]. Thus, an optimal balance is essential.

(4) Integrated effects and mechanistic control

The interplay among defects, dopants, and surface functionalities determines the dominant reaction pathway. For instance, nitrogen-doped sludge-derived biochar simultaneously contains defects, surface functional groups, and heteroatom dopants. However, the dominant reactive species varied with the pyrolysis temperature: the contribution of free radicals to sulfamethoxazole degradation gradually decreased as the calcination temperature increased from 300 to 800 °C, whereas the contribution of surface-bound reactive species increased correspondingly. Nonetheless, correlation analysis revealed that the degradation rate of sulfamethoxazole was not proportional to the defect degree, nitrogen content, or oxygen-containing functional groups individually, indicating that defects, dopants, and surface functionalities collectively determine the PMS activation pathway [160]. In general, carbon-based materials typically possess multiple active sites that collectively govern the persulfate activation pathway. Through rational surface design, carbon catalysts can be tailored to achieve tunable redox properties and reaction pathways for sustainable water purification applications [89,161].

4.3. Reaction Condition Regulation

(1) Effects of temperature and solution pH

The solution pH and reaction temperature are crucial environmental factors that govern persulfate activation efficiency and oxidation mechanisms. While their effects on homogeneous systems are well understood [162], their influence on heterogeneous catalytic systems is more complex, as both parameters not only affect persulfate decomposition kinetics but also regulate the surface charge, active site state, and electron transfer behavior of the catalyst [163].

Temperature plays a dual role in heterogeneous persulfate activation: it directly accelerated persulfate decomposition and indirectly altered the physicochemical properties of the catalyst surface [164,165]. Increasing temperature enhances the intrinsic reaction kinetics and facilitates the formation of ROS. For example, N-doped biochar and graphene materials exhibited significantly higher activation rates at elevated temperatures due to accelerated electron transfer and reduced activation energy [166].

The solution pH profoundly affects not only the speciation of persulfate but also the surface charge state, electron distribution, and adsorption characteristics of carbon-based catalysts [32]. Taken carbon-based materials as examples, at low pH, the carbon surface tended to become positively charged, favoring the adsorption of negatively charged persulfate anions and facilitating electron transfer reactions [167]. In this environment, $SO_4^{\bullet-}$ is usually the dominant ROS, leading to radical-based oxidation pathways [168]. In contrast, at neutral to alkaline pH, several effects emerged. First, the carbon surface becomes negatively charged, which may electrostatically repel persulfate anions, decreasing their adsorption and activation efficiency [169]. Secondly, due to the increased content of hydroxyl ions, $SO_4^{\bullet-}$ would be converted into •OH, and partial •OH will be quenched by hydroxyl ions

[170]. Thirdly, certain functionalized or doped carbon materials (e.g., graphitic N-doped carbons) can maintain high activity even under alkaline conditions, as the non-radical electron transfer pathway or $^1O_2$-based oxidation dominates [171]. Furthermore, pH affects the ionization state of surface oxygen groups (e.g., -COOH ↔ -COO^-), which changes the adsorption affinity for both persulfate and organic pollutants [172]. An optimal pH is thus critical to balance surface adsorption, radical generation, and non-radical activation efficiency.

The combined influence of pH and temperature dictates the predominant reaction pathway and ROS composition. For instance, carbonaceous catalysts with abundant C=O and graphitic N sites have been shown to exhibit enhanced $^1O_2$ production under alkaline and warm conditions, leading to higher selectivity and reduced mineralization energy [92].

Understanding and optimizing these environmental factors are therefore essential for maximizing the catalytic performance and stability of heterogeneous catalysts in persulfate-based AOPs.

(2) Influence of coexisting ions and dissolved organic matter

In addition to their effects in homogeneous persulfate activation systems, inorganic anions also affect heterogeneous persulfate activation on catalyst surfaces by interacting with surface active sites, modifying adsorption behavior, and altering reactive-species generation. For example, chloride ions present in the reaction solution can adsorb on carbon catalyst surfaces and change surface charge or passivate defect/edge sites, which may inhibit or alter the pathway of persulfate activation by reducing access of persulfate molecules to these active sites [173]. In some cases, however, chloride ions may promote secondary radical formation (e.g., chlorine radicals) that propagate persulfate decomposition on surfaces, increasing oxidative performance [153]. Bicarbonate/carbonate ions can adsorb onto carbon surfaces and compete with persulfate or pollutants for adsorption sites, thus reducing the local concentration of persulfate at the catalyst interface and diminishing activation efficiency [174]. Moreover, these anions may scavenge intermediate radicals near the material surface and thereby suppress non-radical pathways [175]. In biochar- or activated carbon-based persulfate systems, for instance, high concentrations of phosphate have been shown to strongly inhibit degradation, likely due to the adsorption of phosphate onto the carbon surface blocking active ketone or carbonyl (C=O) sites required for surface-mediated activation [176]. In summary, while inorganic anions may act merely as scavengers in bulk solution, their presence in heterogeneous carbon-persulfate systems can exert additional adverse effects by interfering with the catalyst surface structure, adsorption equilibria and reactive-species generation pathways, thereby altering the apparent tolerance of the material toward matrix anions.

Dissolved organic matter such as humic acid in water has been shown to have significant effects on persulfate activation systems, which can either promote or inhibit the activation process depending on the specific conditions and reaction mechanisms. For instance, humic acid promoted PMS activation for the degradation of bisphenol A [177], while humic acid inhibited PMS activation for the degradation of sulfamethoxazole [178].

When considering the oxidation efficiency of different persulfate-based systems, the order of effectiveness varies significantly. Research has indicated that for peroxide oxidants, the oxidation efficiency generally follows the sequence of O_3/MnO_2 > PMS/MnO_2 > PDS/MnO_2 > H_2O_2/MnO_2 [179]. This suggests that the choice of oxidant and catalyst combination plays a crucial role in determining the overall effectiveness of the system, especially in the presence of complex water matrices containing dissolved organic matter.

In general, the interaction between dissolved organic matter and persulfate activation systems can occur through multiple pathways. Dissolved organic matter may act as a radical scavenger, competing with target pollutants for reactive oxygen species generated during persulfate activation. Alternatively, under certain conditions, dissolved organic matter may enhance the activation process by facilitating electron transfer or stabilizing reactive intermediates. The complex nature of dissolved organic matter, which contains various functional groups and molecular structures, contributes to its dual role in persulfate-based AOPs [180].

(3) Synergistic interactions among catalyst, pollutant, and oxidant

Similar to the synergistic effect of different active sites, synergistic interactions among the catalyst, pollutant, and oxidant also play a decisive role in governing the efficiency and pathway of persulfate activation. For instance, in the Fe/N-SAC system, the iron single atoms serve as electron-accepting centers that directly extracted electrons from electron-donating pollutants such as paracetamol or bisphenol A, leading to a reduction in iron valence (e.g., from +2.37 to +2.07) in the absence of oxidants. When PMS is introduced, the system transitions to an external-driven mode where electrons from pollutants are simultaneously transferred to both PMS and iron sites, activating both ETP and radical pathways. The degradation efficiency and mechanism were further modulated by the electron-donating capacity of pollutants, as reflected by their electrophilicity index. For example, pollutants with low electrophilicity indexes (e.g., bisphenol A) favored ETP-dominated oxidation, while those with high electrophilicity indexes (e.g., carbamazepine) relied more on radical pathways. This tripartite synergy is

universally observed in other systems [181]. In addition, Cheng et al. reported that a single-atom Fe-N-C catalyst could generate high-valent iron-oxo species upon PMS activation, which preferentially oxidized sulfamethoxazole via a non-radical pathway, while the same system degraded BPA mainly through a radical mechanism, highlighting how the pollutant's structure steers the reactive species utilization [182]. In another case, Mi et al. demonstrated that by engineering a Co-N_{2+2} coordination structure, the resulting single-atom catalyst almost exclusively produced $^1O_2$ from PMS, which showed superior efficiency in degrading levofloxacin by selectively targeting its electron-rich moieties, a clear synergy between the catalyst's coordination environment and the pollutant's molecular fingerprint [14]. Beyond metal single-atoms, Ren et al. revealed that the surface functional groups on carbon nanotubes could selectively activate PDS into a non-radical pathway, where the electron transfer efficiency was strongly dependent on the redox potential of pollutants like phenol and 4-chlorophenol, showcasing the critical role of the carbon catalyst's electronic properties in mediating the oxidant-pollutant interaction [183]. Collectively, these examples underscore a tunable and efficient degradation paradigm where the catalyst structure dictates electron transfer capacity or reactive species generation, the pollutant regulates electron supply and reaction preference, and the oxidant defines the available reaction channels, enabling the design of advanced oxidation processes tailored to specific contaminants.

5. Challenges and Perspectives in Practical Applications

Despite the promising performance of these catalytic and oxidation systems under laboratory conditions, significant uncertainties remain when they are exposed to complex water environments and long-term operational settings. These factors directly influence their universality, sustainability, and potential for large-scale implementation. To more clearly elucidate the key issues constraining their practical deployment and to explore possible pathways for advancement, the following aspects need to be further considered and investigated.

5.1. Identification of Reactive Species in Complex Water Matrices

To achieve high efficiency in persulfate-based AOPs, it is essential to regulate the reactive species to fully leverage their respective advantages. For instance, •OH is preferable when the wastewater mainly consists of organic pollutants, whereas non-radical species such as $^1O_2$ become important for treating high-salinity wastewater containing chloride ions. These preferences stem from the distinct physicochemical properties of different reactive species discussed in Sections 2 and 4. For example: (1) HO• exhibits high reaction rate constants with a broad range of organics but is susceptible to scavenging by chloride and carbonate ions, making it more suitable for organic-rich, low-salinity matrices; (2) $^1O_2$ operates via a selective, non-radical pathway with longer lifespan and higher tolerance to common anions (Section 2.2.1), thus favoring its use in saline wastewater; (3) surface-bound complexes and high-valent metal-oxo species (Sections 2.2.2 and 2.2.3) show strong resistance to background scavengers and pH variations, making them advantageous for complex or fluctuating water compositions.

However, in real wastewater systems, it is often difficult to obtain accurate information about all matrix components. Therefore, it is crucial to first identify the reactive species under actual wastewater conditions. A major challenge, however, lies in accurately determining the dominant reactive species in complex water matrices, where background constituents such as chlorides, carbonates, and natural organic matter can scavenge reactive species, obscure detection signals, or even generate secondary radicals that alter degradation pathways. For example, although quenching experiments and EPR can reveal the presence of radicals, their quantitative contributions may be misinterpreted, as co-existing substances can suppress or enhance specific pathways, complicating mechanistic analysis. Future progress relies on integrating advanced in-situ spectroscopic techniques, selective probe molecules, and computational modeling to disentangle the complex reaction network. By quantifying the interactions between reactive species and matrix components, more predictive models can be developed to guide catalyst selection and optimize treatment performance for specific wastewater scenarios.

5.2. Understanding the Influence of Water Component Accurately

Understanding the effects of dissolved organic matter on persulfate activation is essential for the practical application of these technologies in real water treatment scenarios. The presence of dissolved organic matter can significantly influence the efficiency, kinetics, and underlying mechanisms of persulfate-based AOP by scavenging reactive species, competing for active sites, or forming secondary intermediates that alter degradation pathways. However, due to its heterogeneous composition and structural complexity, accurately predicting its interactions with reactive species remains a major challenge. Traditional characterization methods often fail to capture the dynamic, multi-step reactions occurring between dissolved organic matter, catalysts, and oxidants.

A similar challenge arises from the presence of inorganic anions in real water matrices. Although numerous laboratory studies have explored the effects of individual anions on persulfate-based AOPs, the behavior of these systems under real wastewater conditions remains difficult to predict. In complex matrices where multiple inorganic anions coexist, their competing scavenging roles, synergistic or antagonistic interactions, and potential to generate secondary radicals can lead to outcomes that deviate significantly from controlled experimental observations. Consequently, the overall influence of inorganic anions on persulfate activation in practical applications is still largely uncertain. This inherent complexity and variability underscore the importance of developing robust, selective non-radical systems such as those based on surface-bound reactive complexes, high-valent metal-oxo species, or direct electron-transfer pathways (Sections 2.2 and 4) which exhibit better tolerance to common background anions and offer more predictable performance in complex water matrices.

Looking ahead, advancing this understanding will require the integration of well-defined model compounds, high-resolution analytical techniques, and kinetic or reactive-transport modeling to disentangle the competing reactions occurring in complex matrices. Developing quantitative structure–activity relationships (QSARs), multiparameter models, or machine-learning frameworks may further enable predictive assessments of both humic acid and inorganic anion effects across different water sources. Such progress will ultimately support the rational design of catalysts and operational strategies that maintain high efficiency and robustness under the diverse and variable conditions encountered in real-world wastewater treatment.

5.3. Catalyst Stability and Reusability

The practical application of advanced catalysts is severely constrained by issues of stability and reusability, primarily due to metal leaching, active site poisoning, or structural collapse under harsh oxidative conditions. For example, although the Fe/N-SAC catalyst demonstrated good stability over multiple cycles, the study usually noted a gradual decline in performance in the internal-driven system, partly due to the need for a higher catalyst loading and the potential for fouling by polymeric products formed during degradation. The future prospect focuses on designing robust catalytic structures with enhanced durability through strategies such as strengthening the metal-support interaction (e.g., creating more stable Fe-N_4 configurations), using protective layers or dopants to shield active sites, or combining with membrane and developing efficient in-situ regeneration protocols.

5.4. Green and Sustainable Catalyst Design Strategies

The traditional synthesis of catalysts often relies on expensive, toxic precursors and energy-intensive processes, conflicting with the environmental goals of the water treatment technologies they enable. The challenge is to develop high-performance catalysts through green chemistry principles, minimizing environmental impacts across their entire life cycle. A promising prospect is the utilization of abundant, low-cost, and renewable biomass waste as catalyst precursors as exemplified by the use of lignin. The future direction involves integrating green synthesis (e.g., using waste-derived materials), minimizing the use of critical metals, and designing systems that operate with low or zero chemical oxidant addition, thereby aligning catalyst production and use with the principles of circular economy and sustainable development.

5.5. Machine Learning and Predictive Modeling for Catalyst and Pathway Design

The integration of machine-learning and computational modeling offers a promising avenue to accelerate the development of persulfate-based AOPs. By learning from experimental and theoretical datasets, machine-learning models can uncover complex, non-linear relationships between catalyst properties, reaction conditions, and system performance. For instance, catalyst descriptors such as coordination number, metal electronegativity, defect density, and doping type can be used as input features to predict the dominant activation pathway or the yield of specific reactive species. Similarly, water matrix parameters including pH, ionic strength, and the concentration of background anions or natural organic matter can be incorporated to forecast degradation efficiency and oxidant utilization in real wastewater. Early applications in related catalytic fields have demonstrated the potential of machine-learning for optimizing Fenton-like systems and predicting catalytic activity from material fingerprints [184,185].

However, a key bottleneck remains the scarcity of standardized, high-quality datasets for persulfate activation systems. Most existing studies are fragmented in terms of experimental conditions, characterization methods, and reporting formats, hindering the construction of robust training databases. Future efforts should prioritize data curation, sharing protocols, and multimodal data integration (combining structural, spectroscopic, kinetic, and computational data). Approaches such as active learning can help overcome data limitations. Ultimately, coupling

machine-learning with mechanistic insights and advanced characterization will enable the rational design of catalysts with tailored activity, selectivity, and stability for specific water treatment scenarios.

6. Conclusions

Persulfate-based AOPs have made significant progress in recent years, driven by the discovery of diverse reactive species and the development of sophisticated catalytic materials. This review demonstrates that the generation of reactive species is not governed by a single factor but rather dictated by the intricate interplay among catalyst structure, surface physicochemical properties, pollutant characteristics, and reaction conditions. Although extensive mechanistic studies have enabled a deeper understanding of radical and non-radical pathways, translating these insights into practical water treatment remains challenging.

A major bottleneck lies in the accurate identification of dominant reactive species in real water matrices. Coexisting inorganic anions, natural organic matter, and variable water chemistries significantly complicate reaction pathways, often leading to misinterpretation when traditional scavenging or probe methods are used alone. Integrating advanced in-situ spectroscopies, isotope-based diagnostics, kinetic modeling, and multi-technique validation will be essential to establish reliable mechanistic fingerprints for complex systems. Another critical issue is the long-term stability and reusability of catalysts. Metal leaching, active site poisoning, and structural degradation continue to hinder large-scale deployment, underscoring the need for rational engineering of robust coordination environments, defect structures, and protective interfaces.

Sustainability considerations must also guide future catalyst design. Conventional synthesis routes are often energy-intensive and rely on scarce or toxic precursors. Green and circular approaches, such as using biomass-derived carbon, earth-abundant metals, and low-temperature synthesis methods, offer promising alternatives. In parallel, data-driven strategies, including machine-learning-assisted prediction and optimization can hold potential to accelerate catalyst discovery and pathway control, although their effective implementation will require improved data availability through standardized experimental protocols and collaborative data-sharing efforts.

To accelerate the transition from laboratory-scale discovery to real-world implementation, several emerging research directions deserve focused attention: (1) in situ catalyst regeneration strategies that mitigate deactivation (e.g., via electrochemical, photochemical, or chemical washing protocols) could extend catalyst lifespan and reduce operational costs; (2) real-time monitoring of reactive species in complex water matrices using advanced in situ spectroscopy, electrochemical sensors, or rapid probe techniques would enable dynamic process control and better mechanistic validation under realistic conditions; (3) machine-learning-guided catalyst design can help identify optimal material descriptors (e.g., coordination environment, defect density, doping type) and predict activation pathways, thereby reducing trial-and-error experimentation; (4) green and circular synthesis routes using waste-derived or earth-abundant precursors should be further developed to align catalyst production with sustainability goals; (5) Integrated predictive models that combine kinetic data, water matrix effects, and catalyst stability parameters are needed to forecast treatment performance across varying water compositions.

Overall, future research should prioritize mechanistic understanding under realistic water chemistries, the development of stable and environmentally benign catalysts, and the establishment of predictive frameworks that bridge fundamental insights with engineered applications. Guided by a rational selection and regulation of reactive species tailored to specific wastewater compositions, these advances will enable persulfate-based AOPs to evolve into reliable, sustainable, and widely deployable technologies for advanced water purification.

Author Contributions

S. W. Conceptualization, formal analysis, writing—original, review & editing. J. W. Conceptualization, supervision and writing—review & editing. All authors have read and agreed to the published version of the manuscript.

Funding

This research was supported by the National Natural Science Foundation of China (52370080).

Institutional Review Board Statement

Not applicable.

Informed Consent Statement

Not applicable.

Data Availability Statement

Data will be made available on request.

Conflicts of Interest

The authors declare no conflict of interest. Given the role as editorial board member, Shizong Wang and editor-in-chief, Jianlong Wang had no involvement in the peer review of this paper and had no access to information regarding its peer-review process. Full responsibility for the editorial process of this paper was delegated to another editor of the journal.

Use of AI and AI-Assisted Technologies

No AI tools were utilized for this paper.

References

1. Ruan, T.; Li, P.; Wang, H.; et al. Identification and prioritization of environmental organic pollutants: From an analytical and toxicological perspective. *Chem. Rev.* **2023**, *123*, 10584–10640.
2. Zhou, W.; Li, M.; Achal, V. A comprehensive review on environmental and human health impacts of chemical pesticide usage. *Emerg. Contam.* **2025**, *11*, 100410.
3. Shi, Y.; Feng, D.; Ahmad, S.; et al. Recent advances in metal–organic frameworks–derived carbon-based materials in sulfate radical-based advanced oxidation processes for organic pollutant removal. *Chem. Eng. J.* **2023**, *454*, 140244.
4. Yu, T.; Chen, H.; Hu, T.; et al. Recent advances in the applications of encapsulated transition-metal nanoparticles in advanced oxidation processes for degradation of organic pollutants: A critical review. *Appl. Catal. B Environ.* **2024**, *342*, 123401.
5. Wang, S.; Wang, J. Electron beam technology coupled to Fenton oxidation for advanced treatment of dyeing wastewater: From laboratory to full application. *ACS EST Water* **2022**, *2*, 852–862.
6. Fareed, A.; Hussain, A.; Nawaz, M.; et al. The impact of prolonged use and oxidative degradation of Atrazine by Fenton and photo-Fenton processes. *Environ. Technol. Innov.* **2021**, *24*, 101840.
7. Wang, N.; Lin, C.; Ren, Z.; et al. Radical and non-radical mechanisms for removal of micropollutants in peroxymonosulfate activation systems: Their generation and identification. *Appl. Catal. B Environ. Energy* **2025**, *383*, 126139.
8. Li, H.; Qin, X.; Wang, K.; et al. Insight into metal-based catalysts for heterogeneous peroxymonosulfate activation: A critical review. *Sep. Purif. Technol.* **2024**, *333*, 125900.
9. Shang, Y.; Xu, X.; Gao, B.; et al. Single-atom catalysis in advanced oxidation processes for environmental remediation. *Chem. Soc. Rev.* **2021**, *50*, 5281–5322.
10. Wang, A.; Zhu, B.-Z.; Huang, C.-H.; et al. Generation mechanism of singlet oxygen from the interaction of peroxymonosulfate and chloride in aqueous systems. *Water Res.* **2023**, *235*, 119904.
11. Wang, Y.; Wang, S.Z.; Liu, Y.; et al. Visible light-enhanced interface interaction for PMS activation towards the removal of emerging organic pollutants: performance, mechanism and toxicity. *Sep. Purif. Technol.* **2025**, *354*, 128741.
12. Wang, S.Z.; Wang, J.L.; Lai, B. Support-modulated coordination environments direct divergent PMS activation pathways in Co single-atom catalysts. *Appl. Catal. B Environ. Energy* **2025**, 125898.
13. Zhu, S.; Huang, X.; Ma, F.; et al. Catalytic removal of aqueous contaminants on N-doped graphitic biochars: Inherent roles of adsorption and nonradical mechanisms. *Environ. Sci. Technol.* **2018**, *52*, 8649–8658.
14. Mi, X.; Wang, P.; Xu, S.; et al. Almost 100% peroxymonosulfate conversion to singlet oxygen on single-atom CoN_{2+2} sites. *Angew. Chem.* **2021**, *133*, 4638–4643.
15. Zhang, X.; Tang, J.; Wang, L.; et al. Nanoconfinement-triggered oligomerization pathway for efficient removal of phenolic pollutants via a Fenton-like reaction. *Nat. Commun.* **2024**, *15*, 917.
16. Garcia-Segura, S.; Qu, X.; Alvarez, P.J.J.; et al. Opportunities for nanotechnology to enhance electrochemical treatment of pollutants in potable water and industrial wastewater–A perspective. *Environ. Sci. Nano* **2020**, *7*, 2178–2194.
17. Tian, D.; Zhou, H.; Zhang, H.; et al. Heterogeneous photocatalyst-driven persulfate activation process under visible light irradiation: From basic catalyst design principles to novel enhancement strategies. *Chem. Eng. J.* **2022**, *428*, 131166.
18. He, S.; Chen, Y.; Li, X.; et al. Heterogeneous photocatalytic activation of persulfate for the removal of organic contaminants in water: A critical review. *Acs EsT Eng.* **2022**, *2*, 527–546.
19. Aziz, K.H.H.; Mustafa, F.S.; Hama, S. Pharmaceutical removal from aquatic environments using multifunctional metal-organic frameworks (MOFs) materials for adsorption and degradation processes: A review. *Coord. Chem. Rev.* **2025**, *542*, 216875.

20. Peng, W.; Dong, Y.; Fu, Y.; et al. Non-radical reactions in persulfate-based homogeneous degradation processes: A review. *Chem. Eng. J.* **2021**, *421*, 127818.
21. Wang, S.Z.; Wang, J.L. Degradation of carbamazepine by radiation-induced activation of peroxymonosulfate. *Chem. Eng. J.* **2018**, *336*, 595–601.
22. Yan, Y.; Wei, Z.; Duan, X.; et al. Merits and limitations of radical vs. nonradical pathways in persulfate-based advanced oxidation processes. *Environ. Sci. Technol.* **2023**, *57*, 12153–12179.
23. Lu, J.; Lu, Q.; Di, L.; et al. Iron-based biochar as efficient persulfate activation catalyst for emerging pollutants removal: A review. *Chin. Chem. Lett.* **2023**, *34*, 108357.
24. Song, H.; Yan, L.; Wang, Y.; et al. Electrochemically activated PMS and PDS: Radical oxidation versus nonradical oxidation. *Chem. Eng. J.* **2020**, *391*, 123560.
25. Weng, Z.; Lin, Y.; Guo, S.; et al. Site engineering of covalent organic frameworks for regulating peroxymonosulfate activation to generate singlet oxygen with 100% selectivity. *Angew. Chem.* **2023**, *135*, e202310934.
26. Zhang, H.; Xie, C.; Chen, L.; et al. Different reaction mechanisms of $SO_4^{\bullet-}$ and •OH with organic compound interpreted at molecular orbital level in Co (II)/peroxymonosulfate catalytic activation system. *Water Res.* **2023**, *229*, 119392.
27. Zhu, Y.; Liu, Y.; Li, P.; et al. A comparative study of peroxydisulfate and peroxymonosulfate activation by a transition metal-H_2O_2 system. *Environ. Sci. Pollut. Res.* **2021**, *28*, 47342–47353.
28. Ma, W.; Ren, X.; Li, J.; et al. Advances in atomically dispersed metal and nitrogen Co-doped carbon catalysts for advanced oxidation technologies and water remediation: From microenvironment modulation to non-radical mechanisms. *Small* **2024**, *20*, 2308957.
29. Das, T.N. Reactivity and role of $SO_5^{\bullet-}$ radical in aqueous medium chain oxidation of sulfite to sulfate and atmospheric sulfuric acid generation. *J. Phys. Chem. A* **2001**, *105*, 9142–9155.
30. Yang, Y.; Jiang, J.; Lu, X.; et al. Production of sulfate radical and hydroxyl radical by reaction of ozone with peroxymonosulfate: A novel advanced oxidation process. *Environ. Sci. Technol.* **2015**, *49*, 7330–7339.
31. Lee, J.; Von Gunten, U.; Kim, J.-H. Persulfate-based advanced oxidation: Critical assessment of opportunities and roadblocks. *Environ. Sci. Technol.* **2020**, *54*, 3064–3081.
32. Liang, J.; Chen, K.; Duan, X.; et al. pH-dependent generation of radical and nonradical species for sulfamethoxazole degradation in different carbon/persulfate systems. *Water Res.* **2022**, *224*, 119113.
33. Zhou, D.; Li, Z.; Hu, X.; et al. Single atom catalyst in persulfate oxidation reaction: From atom species to substance. *Small* **2024**, *20*, 2311691.
34. Zhu, H.; Ma, H.; Zhao, Z.; et al. Electron transfer tuning for persulfate activation via the radical and non-radical pathways with biochar mediator. *J. Hazard. Mater.* **2025**, *486*, 136825.
35. Liu, C.; Ding, Z.; Shi, M.; et al. Dependence of superoxide radical generation on peroxymonosulfate under visible light: Enrofloxacin degradation and mechanism insight. *Chem. Eng. J.* **2024**, *485*, 149721.
36. Furman, O.S.; Teel, A.L.; Watts, R.J. Mechanism of base activation of persulfate. *Environ. Sci. Technol.* **2010**, *44*, 6423–6428.
37. Luo, L.; Han, X.; Wang, K.; et al. Nearly 100% selective and visible-light-driven methane conversion to formaldehyde via. single-atom Cu and $W^{\delta+}$. *Nat. Commun.* **2023**, *14*, 2690.
38. Yu, G.; Wang, Y.; Cao, H.; et al. Reactive oxygen species and catalytic active sites in heterogeneous catalytic ozonation for water purification. *Environ. Sci. Technol.* **2020**, *54*, 5931–5946.
39. Yang, H.; Qiu, R.; Tang, Y.; et al. Carbonyl and defect of metal-free char trigger electron transfer and $O_2^{\bullet-}$ in persulfate activation for Aniline aerofloat degradation. *Water Res.* **2023**, *231*, 119659.
40. Nidheesh, P.V.; Boczkaj, G.; Ganiyu, S.O.; et al. Generation, properties, and applications of singlet oxygen for wastewater treatment: A review. *Environ. Chem. Lett.* **2025**, *23*, 195–240.
41. Tian, C.; Dai, C.; Tian, X.; et al. Effects of Lewis acid-base site and oxygen vacancy in MgAl minerals on peroxymonosulfate activation towards sulfamethoxazole degradation via radical and non-radical mechanism. *Sep. Purif. Technol.* **2022**, *286*, 120437.
42. Tao, Y.; Hou, Y.; Yang, H.; et al. Interlayer synergistic reaction of radical precursors for ultraefficient $^1O_2$ generation via quinone-based covalent organic framework. *Proc. Natl. Acad. Sci. USA* **2024**, *121*, e2401175121.
43. Yi, Q.; Ji, J.; Shen, B.; et al. Singlet oxygen triggered by superoxide radicals in a molybdenum cocatalytic Fenton reaction with enhanced REDOX activity in the environment. *Environ. Sci. Technol.* **2019**, *53*, 9725–9733.
44. Gao, Y.; Chen, Z.; Zhu, Y.; et al. New insights into the generation of singlet oxygen in the metal-free peroxymonosulfate activation process: Important role of electron-deficient carbon atoms. *Environ. Sci. Technol.* **2019**, *54*, 1232–1241.
45. Hu, H.; Chen, D.; Liang, Y.; et al. Understanding the active sites and associated reaction pathways of metal-free carbocatalysts in persulfate activation and pollutant degradation. *Environ. Sci. Nano* **2024**, *11*, 1368–1393.
46. Zhao, H.-Q.; Song, J.-S.; Lu, P.; et al. Single atom Co-anchored nitrogen-doped graphene for peroxymonosulfate activation with high selectivity of singlet oxygen generation. *Chem. Eng. J.* **2023**, *456*, 141045.
47. Ali, J.; Zhan, K.; Wang, H.; et al. Tuning of persulfate activation from a free radical to a nonradical pathway through the

incorporation of non-redox magnesium oxide. *Environ. Sci. Technol.* **2020**, *54*, 2476–2488.
48. Wei, Y.; Miao, J.; Cui, J.; et al. Heteroatom substitution enhances generation and reactivity of surface-activated peroxydisulfate complexes for catalytic Fenton-like reactions. *J. Hazard. Mater.* **2024**, *467*, 133753.
49. Chen, J.; Zhou, X.; Sun, P.; et al. Complexation enhances Cu (II)-activated peroxydisulfate: A novel activation mechanism and Cu (III) contribution. *Environ. Sci. Technol.* **2019**, *53*, 11774–11782.
50. Wang, X.; Li, W.; Zhang, J.; et al. The critical roles of surface-bound radicals in the nickel phosphide/biochar-persulfate catalytic oxidation system for tetracycline removal: The synergistic catalysis between nickel phosphides and biochar. *Chem. Eng. J.* **2024**, *491*, 151915. https://doi.org/10.1016/j.cej.2024.151915.
51. Chen, J.; Dong, L.; Huang, S.; et al. Underestimated role of surface-bound peroxymonosulfate and overestimated role of $SO_4^{\bullet-}$and $^1O_2$ in peroxymonosulfate activation with metal oxides. *J. Phys. Chem. C* **2025**, *129*, 20573-20582
52. Fan, Y.; Zhang, Q.; Peng, Y.; et al. Activation of high-valent metal oxidants on carbon catalysts: Mechanisms, applications and challenges. *ACS EST Eng.* **2025**, *5*, 1338-1356
53. He, Y.; Qin, H.; Wang, Z.; et al. Fe-Mn oxycarbide anchored on N-doped carbon for enhanced Fenton-like catalysis: Importance of high-valent metal-oxo species and singlet oxygen. *Appl. Catal. B Environ.* **2024**, *340*, 123204.
54. Wang, S.Z; Wang, J.L. Single atom cobalt catalyst derived from co-pyrolysis of vitamin B12 and graphitic carbon nitride for PMS activation to degrade emerging pollutants. *Appl. Catal. B Environ.* **2023**, *321*, 122051.
55. Zhou, H.; He, Y.-l.; Peng, J.; et al. High-valent metal-oxo species transformation and regulation by co-existing chloride: Reaction pathways and impacts on the generation of chlorinated by-products. *Water Res.* **2024**, *257*, 121715.
56. Sen, A.; Sharma, S.; Rajaraman, G. Bridging the oxo wall: A new perspective on high-valent metal-oxo species and their reactivity in Mn, Fe, and Co complexes. *Angew. Chem. Int. Ed.* **2025**, *64*, e202419953.
57. Wang, C.; Xiao, J. Activation of molecular oxygen and selective oxidation with metal complexes. *Acc. Chem. Res.* **2025**, *58*, 714–731.
58. Tang, L.; Liu, Y.; Wang, J.; et al. Enhanced activation process of persulfate by mesoporous carbon for degradation of aqueous organic pollutants: Electron transfer mechanism. *Appl. Catal. B Environ.* **2018**, *231*, 1–10.
59. Ming, H.; Bian, X.; Cheng, J.; et al. Carbon nitride with a tailored electronic structure toward peroxymonosulfate activation: A direct electron transfer mechanism for organic pollutant degradation. *Appl. Catal. B Environ.* **2024**, *341*, 123314.
60. Ren, W.; Cheng, C.; Shao, P.; et al. Origins of electron-transfer regime in persulfate-based nonradical oxidation processes. *Environ. Sci. Technol.* **2021**, *56*, 78–97.
61. Wang, B.; Zhu, E.; Tang, S.; et al. Peroxymonosulfate activation by molybdenum carbide for water decontamination: Key role of surface activated complex. *Chem. Eng. J.* **2025**, *508*, 160980.
62. Zhao, Y.; Yu, L.; Song, C.; et al. Selective degradation of electron-rich organic pollutants induced by CuO@ Biochar: The key role of outer-sphere interaction and singlet oxygen. *Environ. Sci. Technol.* **2022**, *56*, 10710–10720.
63. Duan, P.; Li, M.; Xu, X.; et al. Understanding of interfacial molecular interactions and inner-sphere reaction mechanism in heterogeneous Fenton-like catalysis on Mn-N4 site. *Appl. Catal. B Environ. Energy* **2024**, *344*, 123619.
64. Huang, M.; Han, Y.; Xiang, W.; et al. In situ-formed phenoxyl radical on the CuO surface triggers efficient persulfate activation for phenol degradation. *Environ. Sci. Technol.* **2021**, *55*, 15361–15370.
65. Yang, P.; Tang, J.; Ding, Z.; et al. Sp-hybridized carbon-facilitated peroxymonosulfate activation for superior phenolic pollutant removal. *J. Hazard. Mater.* **2025**, *490*, 137843.
66. Ren, W.; Nie, G.; Zhou, P.; et al. The intrinsic nature of persulfate activation and N-doping in carbocatalysis. *Environ. Sci. Technol.* **2020**, *54*, 6438–6447.
67. Wang, Y.; Liu, Y.; Zhang, H.; et al. Carbonaceous materials in structural dimensions for advanced oxidation processes. *Chem. Soc. Rev.* **2025**, *54*, 2436–2482
68. Peng, J.; Zhou, P.; Zhou, H.; et al. Insights into the electron-transfer mechanism of permanganate activation by graphite for enhanced oxidation of sulfamethoxazole. *Environ. Sci. Technol.* **2021**, *55*, 9189–9198.
69. Zhou, Q.; Song, C.; Wang, P.; et al. Generating dual-active species by triple-atom sites through peroxymonosulfate activation for treating micropollutants in complex water. *Proc. Natl. Acad. Sci. USA* **2023**, *120*, e2300085120.
70. Yin, R.; Guo, W.; Wang, H.; et al. Selective degradation of sulfonamide antibiotics by peroxymonosulfate alone: Direct oxidation and nonradical mechanisms. *Chem. Eng. J.* **2018**, *334*, 2539–2546.
71. Buxton, G.V.; Greenstock, C.L.; Phillips Helman, W.; et al. Critical review of rate constants for reacitons of hydrated electrons. *J. Phys. Chem. Ref. Data* **1988**, *17*. https://doi.org/10.1063/1.555805
72. Haag, W.R.; Gassman, E. Singlet oxygen in surface waters—Part I: Furfuryl alcohol as a trapping agent. *Chemosphere* **1984**, *13*, 631–640.
73. Wang, S.Z.; Liu, Y.; Wang, J.L. Peroxymonosulfate activation by Fe–Co–O-codoped graphite carbon nitride for degradation of sulfamethoxazole. *Environ. Sci. Technol.* **2020**, *54*, 10361–10369.
74. Sun, Z.; Zhao, M.; Zhou, X. Reliability analysis of NaN_3 as quencher of $^1O_2$ in heterogeneous persulfate catalytic

oxidation system. *Catal. Commun.* **2023**, *183*, 106774.
75. Wang, H.; Song, Y.; Xiong, J.; et al. Highly selective oxidation of furfuryl alcohol over monolayer titanate nanosheet under visible light irradiation. *Appl. Catal. B Environ.* **2018**, *224*, 394–403.
76. Zong, Y.; Guan, X.; Xu, J.; et al. Unraveling the overlooked involvement of high-valent cobalt-oxo species generated from the cobalt (II)-activated peroxymonosulfate process. *Environ. Sci. Technol.* **2020**, *54*, 16231–16239.
77. Pan, Q.; Wang, C.; Zhan, P.; et al. Generation and regulation of high-valent metal species in advanced oxidation processes. *Environ. Funct. Mater.* **2025**, *4*, 1–10.
78. Lei, Y.; Yu, Y.; Lei, X.; et al. Assessing the use of probes and quenchers for understanding the reactive species in advanced oxidation processes. *Environ. Sci. Technol.* **2023**, *57*, 5433–5444.
79. Cai, L.; Yao, Q.; Du, X.; et al. Identification of superoxide contribution through the quenching method and model system. *ACS EST Eng.* **2024**, *4*, 2145–2154.
80. Wang, S.Z.; Xu, L.J.; Wang, J.L. Iron-based dual active site-mediated peroxymonosulfate activation for the degradation of emerging organic pollutants. *Environ. Sci. Technol.* **2021**, *55*, 15412–15422.
81. Zong, Y.; Chen, L.; Zeng, Y.; et al. Do we appropriately detect and understand singlet oxygen possibly generated in advanced oxidation processes by electron paramagnetic resonance spectroscopy? *Environ. Sci. Technol.* **2023**, *57*, 9394–9404.
82. Zhang, C.; Liu, X.; Jiang, M.; et al. A review on identification, quantification, and transformation of active species in SCR by EPR spectroscopy. *Environ. Sci. Pollut. Res.* **2023**, *30*, 28550–28562.
83. Chen, L.; Duan, J.; Du, P.; et al. Accurate identification of radicals by in-situ electron paramagnetic resonance in ultraviolet-based homogenous advanced oxidation processes. *Water Res.* **2022**, *221*, 118747.
84. Radi, R. Oxygen radicals, nitric oxide, and peroxynitrite: Redox pathways in molecular medicine. *Proc. Natl. Acad. Sci. USA* **2018**, *115*, 5839–5848.
85. Bakker, M.G.; Fowler, B.; Bowman, M.K.; et al. Experimental methods in chemical engineering: Electron paramagnetic resonance spectroscopy-EPR/ESR. *Can. J. Chem. Eng.* **2020**, *98*, 1668–1681.
86. Cai, J.; Niu, T.; Shi, P.; et al. Boron-doped diamond for hydroxyl radical and sulfate radical anion electrogeneration, transformation, and voltage-free sustainable oxidation. *Small* **2019**, *15*, 1900153.
87. Liao, J.; Li, K.; Ma, H.; et al. Oxygen vacancies on the BiOCl surface promoted photocatalytic complete NO oxidation via superoxide radicals. *Chin. Chem. Lett.* **2020**, *31*, 2737–2741.
88. Mendoza, C.; Désert, A.; Khrouz, L.; et al. Heterogeneous singlet oxygen generation: In-operando visible light EPR spectroscopy. *Environ. Sci. Pollut. Res.* **2021**, *28*, 25124–25129.
89. Wang, J.; Shen, S.; Li, X.; et al. Photoexcited active radicals for environmental and energy applications: Generation, regulation, and dynamic tracking. *Chem. Rev.* **2025**, *125*, 7811–7917.
90. Nikam, R.; Chattopadhyay, A. A computational investigation on the photochemistry of the popular spin-trap agent N-tert-butyl-α-phenylnitrone (PBN) and thermal isomerization pathways of its photoproduct oxaziridine. *Int. J. Quantum Chem.* **2024**, *124*, e27369.
91. Yang, S.; Sun, S.; Xie, Z.; et al. Comprehensive insight into the common organic radicals in advanced oxidation processes for water decontamination. *Environ. Sci. Technol.* **2024**, *58*, 19571–19583.
92. Wang, P.; Zhang, L.; Wang, C.; et al. Inherent persistent free radicals in nonextractable contaminated soil residue driven nontarget reactions and phenolic polymerization in H_2O_2-based in situ remediation. *Environ. Sci. Technol.* **2025**, *59*, 20665–20674.
93. Grajewski, J.; Zgorzelak, M.; Janiak, A.; et al. Controlled, sunlight-driven reversible cycloaddition of multiple singlet oxygen molecules to anthracene-containing trianglimine macrocycles. *Chempluschem* **2022**, *87*, e202100510.
94. Charbouillot, T.; Brigante, M.; Mailhot, G.; et al. Performance and selectivity of the terephthalic acid probe for OH as a function of temperature, pH and composition of atmospherically relevant aqueous media. *J. Photochem. Photobiol. A Chem.* **2011**, *222*, 70–76.
95. Shen, T.; Su, W.; Yang, Q.; et al. Synergetic mechanism for basic and acid sites of MgM_xO_y (M = Fe, Mn) double oxides in catalytic ozonation of p-hydroxybenzoic acid and acetic acid. *Appl. Catal. B Environ.* **2020**, *279*, 119346.
96. Wang, J.; Xu, M.; Liang, X.; et al. Development of a novel 2D Ni-MOF derived NiO@ C nanosheet arrays modified Ti/TiO_2NTs/PbO_2 electrode for efficient electrochemical degradation of salicylic acid wastewater. *Sep. Purif. Technol.* **2021**, *263*, 118368.
97. Kim, M.S.; Lee, C.; Kim, J.-H. Occurrence of unknown reactive species in UV/H_2O_2 system leading to false interpretation of hydroxyl radical probe reactions. *Water Res.* **2021**, *201*, 117338.
98. Le, H.T.; Nguyen, D.P.L.; Shin, H.S.; et al. Chemistry of the carboxylic acid of dihydrofluorescein in oxidation and its application to fluorogenic ROS sensing. *Free Radic. Res.* **2021**, *55*, 461–468.
99. Wang, M.; Ma, J.; Liu, H.; et al. Sustainable productions of organic acids and their derivatives from biomass via selective oxidative cleavage of C–C bond. *ACS Catal.* **2018**, *8*, 2129–2165.

100. George, C.; Rassy, H.E.; Chovelon, J.M. Reactivity of selected volatile organic compounds (VOCs) toward the sulfate radical (SO_4^{-}). *Int. J. Chem. Kinet.* **2001**, *33*, 539–547.
101. Sim Choi, H.; Woo Kim, J.; Cha, Y.N.; et al. A quantitative nitroblue tetrazolium assay for determining intracellular superoxide anion production in phagocytic cells. *J. Immunoass. Immunochem.* **2006**, *27*, 31–44.
102. Koppenol, W.H.; Van Buuren, K.J.H.; Butler, J.; et al. The kinetics of the reduction of cytochrome c by the superoxide anion radical. *Biochim. Et Biophys. Acta (BBA)-Bioenerg.* **1976**, *449*, 157–168.
103. Benov, L.; Sztejnberg, L.; Fridovich, I. Critical evaluation of the use of hydroethidine as a measure of superoxide anion radical. *Free Radic. Biol. Med.* **1998**, *25*, 826–831.
104. Bedouhène, S.; Moulti-Mati, F.; Hurtado-Nedelec, M.; et al. Luminol-amplified chemiluminescence detects mainly superoxide anion produced by human neutrophils. *Am. J. Blood Res.* **2017**, *7*, 41.
105. Chen, Y.; Zhao, C.; Li, Y.; et al. Nitrogen-doped carbon modified with boron atoms activating peroxydisulfate for sulfamethoxazole degradation: The electron transfer-dominated pathway. *J. Environ. Chem. Eng.* **2025**, *13*, 116080. https://doi.org/10.1016/j.jece.2025.116080.
106. Huang, K.Z.; Zhang, H. Galvanic oxidation processes (GOPs): An effective direct electron transfer approach for organic contaminant oxidation. *Sci. Total Environ.* **2020**, *743*, 140828.
107. Zhang, Z.; Zang, Z.; Guo, J.; et al. High-temporal-resolution in situ sensor for oceanic CO_2 isotope measurement enabling multidimensional isotope tracing analysis ($R^{13}C$, $R^{18}O$, and $R^{17}O$) via laser absorption spectroscopy. *Anal. Chem.* **2024**, *96*, 1195–1204.
108. Min, N.; Yao, J.; Wu, L.; et al. Isotope fractionation of diethyl phthalate during oxidation degradation by persulfate activated with zero-valent iron. *Chem. Eng. J.* **2022**, *435*, 132132.
109. Wang, A.; Wang, W.; Xu, J.; et al. Enhancing oxygen evolution reaction by simultaneously triggering metal and lattice oxygen redox pair in iridium loading on Ni-Doped Co_3O_4. *Adv. Energy Mater.* **2023**, *13*, 2302537.
110. Lin, Y.; Yu, L.; Tang, L.; et al. In situ identification and time-resolved observation of the interfacial state and reactive intermediates on a cobalt oxide nanocatalyst for the oxygen evolution reaction. *ACS Catal.* **2022**, *12*, 5345–5355.
111. Ma, F.; Fu, J.; Zhang, J.; et al. Structural tailoring of carbon-based catalysts for persulfate activation toward emerging contaminant remediation: Performance, mechanisms, and applications. *J. Environ. Chem. Eng.* **2025**, *14*, 120780.
112. Zhang, R.; Li, Q.; Du, H.; et al. A review on the correlation among active sites, oxidative species, and degradation routes in persulfate activation by carbon-based iron composites for antibiotics oxidation. *Chem. Eng. J.* **2025**, *518*, 164833.
113. Li, F.; Lu, Z.; Li, T.; et al. Origin of the excellent activity and selectivity of a single-atom copper catalyst with unsaturated Cu-N_2 sites via peroxydisulfate activation: Cu (III) as a dominant oxidizing species. *Environ. Sci. Technol.* **2022**, *56*, 8765–8775.
114. Wang, S.Z.; Wang, J.L.; Xu, H. Discrepant catalytic activity of biochar-based Fe and Co homonuclear and heteronuclear diatomic catalysts for activating peroxymonosulfate to degrade emerging pollutants. *ACS EST Eng.* **2024**, *4*, 1758–1768.
115. He, C.; Zhang, Z.; Wang, J.; et al. Mn–Ce bicenter of a dual single-atom catalyst synergistically triggers reactive oxygen species generation for efficient ozonation of emerging contaminants. *ACS EST Eng.* **2024**, *4*, 2002–2014.
116. Yin, Y.; Lv, R.; Zhang, W.; et al. Exploring mechanisms of different active species formation in heterogeneous Fenton systems by regulating iron chemical environment. *Appl. Catal. B Environ.* **2021**, *295*, 120282. https://doi.org/10.1016/j.apcatb.2021.120282.
117. Wang, S.Z.; Wang, J.L. Cobalt-silicon coordination-induced nonradical activation of peroxymonosulfate for enhancing the degradation of organic pollutants in real wastewater. *Small* **2025**, *21*, 2500434. https://doi.org/10.1002/smll.202500434.
118. Kang, H.; Chen, Y.; Cheng, M.; et al. State-of-the-art structural regulation methods and quantum chemistry for carbon-based single-atom catalysts in advanced oxidation process: Critical perspectives into molecular level. *Adv. Mater.* **2025**, *37*, 2505128. https://doi.org/10.1002/adma.202505128.
119. Song, J.; Hou, N.; Liu, X.; et al. Asymmetrically coordinated CoB_1N_3 moieties for selective generation of high-valence Co-Oxo species via coupled electron–proton transfer in fenton-like reactions. *Adv. Mater.* **2023**, *35*, 2209552.
120. Li, X.; Wen, X.; Lang, J.; et al. CoN_1O_2 single-atom catalyst for efficient peroxymonosulfate activation and selective cobalt (IV) = O generation. *Angew. Chem.* **2023**, *135*, e202303267.
121. Wang, X.; Xiong, Z.; Shi, H.; et al. Switching the reaction mechanisms and pollutant degradation routes through active center size-dependent Fenton-like catalysis. *Appl. Catal. B Environ.* **2023**, *329*, 122569. https://doi.org/10.1016/j.apcatb.2023.122569.
122. Tang, L.; Zhou, D.; Hu, J.; et al. Emerging investigator series: Recent progress on the activation of persulfate by vacancy defect materials: The role of vacancies. *Environ. Sci. Nano* **2024**, *11*, 3230–3249.
123. Muhammad, P.; Zada, A.; Rashid, J.; et al. Defect engineering in nanocatalysts: From design and synthesis to applications. *Adv. Funct. Mater.* **2024**, *34*, 2314686.
124. Chen, S.; Li, J.; Zhou, W.; et al. Engineering defects in heterogeneous catalytic persulfates for water purification: An

overlooked role? *Coord. Chem. Rev.* **2024**, *507*, 215749.
125. Pan, M.; Tang-Hu, S.-Y.; Li, C.; et al. Oxygen vacancy-mediated peroxydisulfate activation and singlet oxygen generation toward 2, 4-dichlorophenol degradation on specific CuO_{1-x} nanosheets. *J. Hazard. Mater.* **2023**, *441*, 129944.
126. Wang, M.-M.; Liu, L.-J.; Xi, J.-R.; et al. Lattice doping of Zn boosts oxygen vacancies in Co_3O_4 nanocages: Improving persulfate activation via forming surface-activated complex. *Chem. Eng. J.* **2023**, *451*, 138605.
127. Bu, Y.; Li, H.; Yu, W.; et al. Peroxydisulfate activation and singlet oxygen generation by oxygen vacancy for degradation of contaminants. *Environ. Sci. Technol.* **2021**, *55*, 2110–2120.
128. Zhao, Y.; Zhang, B.; Xia, B.; et al. Defect engineering boosted peroxydisulfate activation of dual-vacancy Cu–Fe spinel oxides for soil organics decontamination. *ACS EST Eng.* **2024**, *4*, 2025–2035. https://doi.org/10.1021/acsestengg.4c00195.
129. Qin, J.; Duan, M.; Zhang, Y.; et al. Nitrogen-vacancy-rich Co_3O_4/carbon nitride activating peroxymonosulfate for efficient micropollutant degradation: Dominant role of superoxide radicals. *Environ. Res.* **2025**, *285*, 122460.
130. Wang, Q.; Lu, J.; Yu, M.; et al. Sulfur vacancy rich MoS_2/$FeMoO_4$ composites derived from MIL-53 (Fe) as PMS activator for efficient elimination of dye: Nonradical $^1O_2$ dominated mechanism. *Environ. Pollut.* **2023**, *333*, 121990.
131. Yu, S.; Peng, Y.; Shao, P.; et al. Electron-transfer-based peroxymonosulfate activation on defect-rich carbon nanotubes: Understanding the substituent effect on the selective oxidation of phenols. *J. Hazard. Mater.* **2023**, *442*, 130108.
132. Jia, Y.; Yao, X. Defects in carbon-based materials for electrocatalysis: Synthesis, recognition, and advances. *Acc. Chem. Res.* **2023**, *56*, 948–958.
133. Zou, Y.; Wang, S.Z.; Wang, J.L.; et al. Gamma-irradiation induced non-equilibrium defect states in ferric oxychloride promote high-valent iron-oxo pathways for enhanced degradation of sulfamethoxazole from wastewater. *Sep. Purif. Technol.* **2025**, *382*, 136044.
134. Ye, F.; Shi, Y.; Sun, W.; et al. Construction of adsorption-oxidation bifunction-oriented carbon by single boron doping for non-radical antibiotic degradation via persulfate activation. *Chem. Eng. J.* **2023**, *454*, 140148.
135. Qu, G.; Jia, P.; Tang, S.; et al. Enhanced peroxymonosulfate activation via heteroatomic doping defects of pyridinic and pyrrolic N in 2D N-doped carbon nanosheets for BPA degradation. *J. Hazard. Mater.* **2024**, *461*, 132626.
136. Wang, Y.; Zhang, Z.; Yin, Z.; et al. Adsorption and catalysis of peroxymonosulfate on carbocatalysts for phenol degradation: The role of pyrrolic-nitrogen. *Appl. Catal. B Environ.* **2022**, *319*, 121891.
137. Yan, S.; Chen, X.; Yang, Y.; et al. Peroxymonosulfate activation by N-doped 3D graphene from spent lithium-ion batteries for organic pollutants degradation: An insight into the degradation mechanism. *Chem. Eng. J.* **2024**, *484*, 149379.
138. Liu, S.; Pan, Q.; Li, J.; et al. Enhanced mediated electron transfer pathway of peroxymonosulfate activation dominated with graphitic-N for the efficient degradation of various organic contaminants in multiple solutions. *ACS EST Water* **2022**, *2*, 817–829.
139. Li, X.; Chen, X.; Yan, Y.; et al. Nitrogen-doped graphene for tetracycline removal via enhancing adsorption and non-radical persulfate activation. *Environ. Res.* **2023**, *235*, 116642.
140. Zhen, Y.; Zhu, S.; Sun, Z.; et al. Identifying the persistent free radicals (PFRs) formed as crucial metastable intermediates during peroxymonosulfate (PMS) activation by N-doped carbonaceous materials. *Environ. Sci. Technol.* **2021**, *55*, 9293–9304.
141. Duan, X.; Ao, Z.; Sun, H.; et al. Nitrogen-doped graphene for generation and evolution of reactive radicals by metal-free catalysis. *ACS Appl. Mater. Interfaces* **2015**, *7*, 4169–4178. https://doi.org/10.1021/am508416n.
142. Xie, J.; Zhang, L.; Luo, X.; et al. Sulfur anchored on N-doped porous carbon as metal-free peroxymonosulfate activator for tetracycline hydrochloride degradation: Nonradical pathway mechanism, performance and biotoxicity. *Chem. Eng. J.* **2023**, *457*, 141149. https://doi.org/10.1016/j.cej.2022.141149.
143. Liu, B.; Guo, W.; Wang, H.; et al. B-doped graphitic porous biochar with enhanced surface affinity and electron transfer for efficient peroxydisulfate activation. *Chem. Eng. J.* **2020**, *396*, 125119. https://doi.org/10.1016/j.cej.2020.125119.
144. Qi, F.; Zeng, Z.; Wen, Q.; et al. Enhanced organics degradation by three-dimensional (3D) electrochemical activation of persulfate using sulfur-doped carbon particle electrode: The role of thiophene sulfur functional group and specific capacitance. *J. Hazard. Mater.* **2021**, *416*, 125810.
145. Chen, X.; Zhou, Y.; He, J.; et al. Elevated efficiency in tartrazine removal from wastewater through boron-doped biochar: Enhanced adsorption and persulfate activation. *Biochar* **2024**, *6*, 79.
146. Ye, F.; Sun, W.; Pang, K.; et al. Coupling of sulfur and boron in carbonaceous material to strengthen persulfate activation for antibiotic degradation: Active sites, mechanism, and toxicity assessment. *Chin. Chem. Lett.* **2023**, *34*, 107755. https://doi.org/10.1016/j.cclet.2022.107755.
147. Wang, S.; Wang, J. High efficient activation of peroxymonosulfate by Co_9S_8 anchored in N, S, O co-doped carbon composite for degradation of sulfamethoxazole: Effect of sulfur precursor and sulfur doping content. *Chem. Eng. J.* **2022**, *434*, 134824.
148. Ede, S.R.; Luo, Z. Tuning the intrinsic catalytic activities of oxygen-evolution catalysts by doping: A comprehensive

review. *J. Mater. Chem. A* **2021**, *9*, 20131–20163.
149. Gomathi Devi, L.; Narasimha Murthy, B. Characterization of Mo doped TiO_2 and its enhanced photo catalytic activity under visible light. *Catal. Lett.* **2008**, *125*, 320–330.
150. Nie, C.; Dai, Z.; Liu, W.; et al. Criteria of active sites in nonradical persulfate activation process from integrated experimental and theoretical investigations: Boron–nitrogen-co-doped nanocarbon-mediated peroxydisulfate activation as an example. *Environ. Sci. Nano* **2020**, *7*, 1899–1911.
151. Kang, J.; Duan, X.; Wang, C.; et al. Nitrogen-doped bamboo-like carbon nanotubes with Ni encapsulation for persulfate activation to remove emerging contaminants with excellent catalytic stability. *Chem. Eng. J.* **2018**, *332*, 398–408. https://doi.org/10.1016/j.cej.2017.09.102.
152. Yan, Y.; Yang, Q.; Shang, Q.; et al. Ru doped graphitic carbon nitride mediated peroxymonosulfate activation for diclofenac degradation via singlet oxygen. *Chem. Eng. J.* **2022**, *430*, 133174.
153. Wang, S.Z.; Wang, J.L. Active site evolution in cobalt-based catalysts for intensifying water purification: from single-atom to diatomic configurations. *Small Methods* **2025**, *9*, e01565.
154. Miao, F.; Yue, X.; Cheng, C.; et al. Insights into the mechanism of carbocatalysis for peracetic acid activation: Kinetic discernment and active site identification. *Water Res.* **2022**, *227*, 119346.
155. Li, L.; Zhao, J.; Zhao, X.; et al. Insight into the mechanism of peracetic acid activation by corn straw-derived biochar as efficient green activator mediating electron transfer: Crucial role of carbonyl functional group. *Sep. Purif. Technol.* **2025**, *354*, 129005.
156. Wang, M.; Tang, Y.; Wang, J.; et al. Promoted peroxydisulfate activation by nitrogen-doped carbon embedding iron on a nickel foam cathode: Performance, mechanism and relationship between CO and $^1O_2$ generation. *Chem. Eng. J.* **2023**, *460*, 141638.
157. Peng, J.; Wu, E.; Wang, N.; et al. Removal of sulfonamide antibiotics from water by adsorption and persulfate oxidation process. *J. Mol. Liq.* **2019**, *274*, 632–638.
158. Nie, C.; Dai, Z.; Wan, L.; et al. Interfacial electric field tuning carbon-catalyzed persulfate activation toward a maneuverable oxidation pathway for enhanced removal of Bisphenol A. *ACS EST Water* **2023**, *3*, 3004–3014.
159. Forouzesh, M.; Ebadi, A.; Aghaeinejad-Meybodi, A.; et al. Transformation of persulfate to free sulfate radical over granular activated carbon: Effect of acidic oxygen functional groups. *Chem. Eng. J.* **2019**, *374*, 965–974. https://doi.org/10.1016/j.cej.2019.05.220.
160. Wang, S.; Wang, J. Nitrogen doping sludge-derived biochar to activate peroxymonosulfate for degradation of sulfamethoxazole: Modulation of degradation mechanism by calcination temperature. *J. Hazard. Mater.* **2021**, *418*, 126309.
161. Zhang, L.; Lin, C.Y.; Zhang, D.; et al. Guiding principles for designing highly efficient metal-free carbon catalysts. *Adv. Mater.* **2019**, *31*, 1805252.
162. Li, W.; Orozco, R.; Camargos, N.; et al. Mechanisms on the impacts of alkalinity, pH, and chloride on persulfate-based groundwater remediation. *Environ. Sci. Technol.* **2017**, *51*, 3948–3959.
163. Li, P.; Jiao, Y.; Ruan, Y.; et al. Revealing the role of double-layer microenvironments in pH-dependent oxygen reduction activity over metal-nitrogen-carbon catalysts. *Nat. Commun.* **2023**, *14*, 6936.
164. Duan, X.; Sun, H.; Kang, J.; et al. Insights into heterogeneous catalysis of persulfate activation on dimensional-structured nanocarbons. *Acs Catal.* **2015**, *5*, 4629–4636.
165. Fagan, W.P.; Villamena, F.A.; Zweier, J.L.; et al. In situ EPR spin trapping and competition kinetics demonstrate temperature-dependent mechanisms of synergistic radical production by ultrasonically activated persulfate. *Environ. Sci. Technol.* **2022**, *56*, 3729–3738.
166. Duan, X.; Indrawirawan, S.; Kang, J.; et al. Synergy of carbocatalytic and heat activation of persulfate for evolution of reactive radicals toward metal-free oxidation. *Catal. Today* **2020**, *355*, 319–324.
167. Koper, M.T.M. Theory of multiple proton–electron transfer reactions and its implications for electrocatalysis. *Chem. Sci.* **2013**, *4*, 2710–2723.
168. Liang, C.; Su, H.-W. Identification of sulfate and hydroxyl radicals in thermally activated persulfate. *Ind. Eng. Chem. Res.* **2009**, *48*, 5558–5562.
169. Szabó, T.; Tombácz, E.; Illés, E.; et al. Enhanced acidity and pH-dependent surface charge characterization of successively oxidized graphite oxides. *Carbon* **2006**, *44*, 537–545.
170. Wacławek, S.; Lutze, H.V.; Sharma, V.K.; et al. Revisit the alkaline activation of peroxydisulfate and peroxymonosulfate. *Curr. Opin. Chem. Eng.* **2022**, *37*, 100854.
171. Luo, Y.; He, G.; Zhu, Y.; et al. Graphdiyne-mediated non-radical activation originate fast electron transfer for efficient organics removal. *Chem. Eng. J.* **2025**, *509*, 161457.
172. Bandosz, T.J. Surface chemistry of carbon materials. In *Carbon Materials for Catalysis*; John Wiley & Sons, Inc.: Hoboken, NJ, USA, 2008; pp. 45–92.

173. Mubita, T.M.; Dykstra, J.E.; Biesheuvel, P.M.; et al. Selective adsorption of nitrate over chloride in microporous carbons. *Water Res.* **2019**, *164*, 114885.
174. Feng, H.; Li, X.; Xing, Y.; et al. Adsorption of CO_3^{2-}/HCO_3^- on a quartz surface: Cluster formation, pH effects, and mechanistic aspects. *Phys. Chem. Chem. Phys.* **2023**, *25*, 7951–7964.
175. Patra, S.G.; Mizrahi, A.; Meyerstein, D. The role of carbonate in catalytic oxidations. *Acc. Chem. Res.* **2020**, *53*, 2189–2200.
176. Wu, X.; Radovic, L.R. Inhibition of catalytic oxidation of carbon/carbon composites by phosphorus. *Carbon* **2006**, *44*, 141–151.
177. Jia, J.; Liu, D.; Tian, J.; et al. Visible-light-excited humic acid for peroxymonosulfate activation to degrade bisphenol A. *Chem. Eng. J.* **2020**, *400*, 125853.
178. Wang, S.; Wang, J. Synergistic effect of PMS activation by Fe_0@Fe_3O_4 anchored on N, S, O co-doped carbon composite for degradation of sulfamethoxazole. *Chem. Eng. J.* **2022**, *427*, 131960.
179. Ma, J.; Zhang, S.; Duan, X.; et al. Catalytic oxidation of sulfachloropyridazine by MnO_2: Effects of crystalline phase and peroxide oxidants. *Chemosphere* **2021**, *267*, 129287.
180. Luo, D.; Lin, H.; Li, X.; et al. The dual role of natural organic matter in the degradation of organic pollutants by persulfate-based advanced oxidation processes: A mini-review. *Toxics* **2024**, *12*, 770.
181. Guo, J.; Wang, Y.; Shang, Y.; et al. Fenton-like activity and pathway modulation via single-atom sites and pollutants comediates the electron transfer process. *Proc. Natl. Acad. Sci. USA* **2024**, *121*, e2313387121.
182. Cheng, C.; Ren, W.; Miao, F.; et al. Generation of FeIV = O and its contribution to Fenton-like reactions on a single-atom iron− N− C catalyst. *Angew. Chem. Int. Ed.* **2023**, *62*, e202218510.
183. Ren, W.; Xiong, L.; Yuan, X.; et al. Activation of peroxydisulfate on carbon nanotubes: Electron-transfer mechanism. *Environ. Sci. Technol.* **2019**, *53*, 14595–14603.
184. Jia, W.; Li, Y.; Chen, C.; et al. Unveiling the fate of metal leaching in bimetal-catalyzed Fenton-like systems: Pivotal role of aqueous matrices and machine learning prediction. *J. Hazard. Mater.* **2024**, *477*, 135291.
185. Ma, S.; Liu, Z.-P. Machine learning for atomic simulation and activity prediction in heterogeneous catalysis: Current status and future. *ACS Catal.* **2020**, *10*, 13213–13226.